A Simple Sub-Optimal Kalman Filter Implementation for a Gyro-Corrected Satellite Attitude Determination System

Anton de Ruiter,*
Carleton University, Ottawa, ON, Canada

This paper presents a simple Kalman filter implementation for correcting gyro-determined satellite attitude estimates with attitude measurements made using external sensors such as sun-sensors, magnetometers, star-trackers, etc. This paper first generalizes a recently developed nonlinear observer for the gyro-corrected attitude determination problem. By implementing the steady-state Kalman filter in the framework of this nonlinear observer, a computationally simple filter is obtained with sub-optimal steady-state performance. This is important for applications where computational power is limited, such as in micro-/nano-satellite applications. Additionally, in the absence of process and measurement noise, this implementation of the Kalman filter is globally stable. The resulting filter uses constant steady-state Kalman filter gains. It is demonstrated that close-to optimal steady-state performance is obtained.

Keywords: spacecraft attitude determination, computational simplicity, sub-optimal filtering

I. Introduction

The attitude determination capability is a critical feature for satellite missions, often requiring high degrees of accuracy. In certain situations, it is very beneficial to use gyros for this purpose, which can provide low noise measurements at a very high rate. However, the attitude as derived by the integration of three rate-gyro measurements has unbounded errors growing with time, due to gyro drift. Hence, the gyro-determined attitude must be corrected by attitude measurements derived from other sensors that have bounded error, e.g., star-trackers, sun sensors, magnetometers, etc. In this paper, these measurements are termed "external" attitude measurements so as to distinguish them from the gyro measurements. Typically, these external attitude measurements are available at a lower rate and are generally much more noisy than the attitude derived from the gyro measurements [1], however as mentioned, the attitude error is bounded. By appropriately combining the external attitude measurements with the attitude derived from the gyro measurements, high bandwidth, low noise attitude estimates can be obtained.

The foundation of many sophisticated methods for the fusion of data from different sensors is the Kalman filter [2,3]. In particular, it can be used to combine the gyro attitude estimates with the external measurements. This filter provides estimates that are optimal in the sense of minimum error variance. There are many variants of the application of this filter to the attitude estimation problem, as well as alternatives such as unscented and particle filters. Reference [3] provides a good survey of these methods. A disadvantage of many of these approaches is that they can be computationally expensive to implement. This makes their use less suitable for satellites containing processors with very limited capacity, e.g., those on board very small satellites such as the joint Japan-Canada JC2Sat mission [4]. Another limitation of these approaches

is that the stability can only be guaranteed locally [3]. Recently, nonlinear observers have been developed for the attitude estimation problem, that are globally stable [5-7]. These observers solve both of the aforementioned problems, since they only require constant gains in order to be implemented. However, good performance under the influence of process and measurement noise is not guaranteed. In this paper, the observer obtained in [5] is generalized, and it is then shown that the steady-state Kalman filter (with constant gains) may be implemented in this framework in closed-loop form [1]. In this way, a filter is obtained which is globally stable, computationally simple to implement, and provides near-optimal steady-state performance.

There are many means by which the external attitude measurements can be obtained [8]. For some examples; a Star-Tracker can provide a three-axis attitude solution, sun sensor and magnetometer measurements can be combined using deterministic methods such as TRIAD or QUEST to obtain a three-axis attitude measurement [8,9], multiple GPS antennas can be installed to obtain a three-axis attitude measurement using carrier phase differential GPS techniques [10]. In this paper, a full three-axis attitude measurement is assumed to be available and the details on how to obtain the external attitude measurements are not considered.

II. Attitude Representation and Gyro Model

There are many different (but equivalent) parameterizations for representing the satellite attitude [11,12], which can be converted from one to another. The rotation matrix itself C_{bI} could be used, as could any other vector parameterization, for example the quaternion, Euler-Rodrigues parameters, Euler angles, etc [12]. The vector $\boldsymbol{\alpha}$ will be used to denote any vector parameterization of the attitude. If the rotation matrix is used, then the attitude kinematics are given by [11]

$$\dot{\mathbf{C}}_{bI} = -\boldsymbol{\omega}^{\times}\mathbf{C}_{bI} \ . \qquad (1)$$

where $\boldsymbol{\omega}^{\times} = \begin{bmatrix} 0 & -\omega_z & \omega_y \\ \omega_z & 0 & -\omega_x \\ -\omega_y & \omega_x & 0 \end{bmatrix}$ represents the cross-product matrix associated with the vector $\boldsymbol{\omega} = \begin{bmatrix} \omega_x & \omega_y & \omega_z \end{bmatrix}^T$. If a vector parameterization is used, the attitude kinematics have the form

$$\dot{\boldsymbol{\alpha}} = \mathbf{W}(\boldsymbol{\alpha})\boldsymbol{\omega} \ , \qquad (2)$$

where the details of the matrix $\mathbf{W}(\boldsymbol{\alpha})$ can be found in [11].

The particular parameterization chosen is irrelevant to the analysis in this paper, and is completely up to the discretion of the designer.

The gyro-provided angular rate measurement is assumed to be given by

---

[*] Assistant Professor, Department of Mechanical and Aerospace Engineering.

$$\boldsymbol{\omega}^m = \boldsymbol{\omega} + \boldsymbol{b}_\omega + \boldsymbol{w}_\omega \quad . \tag{3}$$

where $\boldsymbol{w}_\omega$ is a zero-mean white noise process. The bias is modeled as a random walk process

$$\dot{\boldsymbol{b}}_\omega = \boldsymbol{w}_{b\omega}, \tag{4}$$

where $\boldsymbol{w}_{b\omega}$ is a zero-mean white noise process. This gyro model is often used and is given in [13].

III. External Attitude Measurement

It is assumed that a measurement (external to the rate-gyro sensors) of the attitude is available in some parameterization, which has the equivalent rotation matrix representation given by $\hat{\mathbf{C}}_{bI}^M$. The measurement error denoted by $\delta\mathbf{C}^M$ is a rotation matrix and is defined as in a Multiplicative Extended Kalman Filter [14] such that

$$\hat{\mathbf{C}}_{bI}^M = \delta\mathbf{C}^M \mathbf{C}_{bI} \tag{5}$$

Assuming reasonably good attitude measurements, the rotation corresponding to $\delta\mathbf{C}^M$ is small. It will be convenient to parameterize $\delta\mathbf{C}^M$ by the quaternion $\left(\boldsymbol{\varepsilon}_M, \eta_M\right)$. This parameterization is given by

$$\begin{aligned} \boldsymbol{\varepsilon}_M &= \boldsymbol{a} \sin\frac{\varphi}{2}, \\ \eta_M &= \cos\frac{\varphi}{2}. \end{aligned} \quad . \tag{6}$$

The measurement error, $\delta\mathbf{C}^M$, is then given by (see [11])

$$\delta\mathbf{C}^M = \mathbf{I} + 2\left(\boldsymbol{\varepsilon}_M^\times \boldsymbol{\varepsilon}_M^\times - \eta_M \boldsymbol{\varepsilon}_M^\times\right). \tag{7}$$

Since the error is assumed to be small, the vector part of the quaternion can be treated as white noise, while the scalar part has unit magnitude, ie.

$$\begin{aligned} \boldsymbol{\varepsilon}_M &= \boldsymbol{v}_M, \\ \left|\eta_M\right| &= 1, \end{aligned} \tag{8}$$

so that for small values, the measurement error is approximated by

$$\delta\mathbf{C}^M \approx I - 2\boldsymbol{v}_M^\times \, . \tag{9}$$

IV. Gyro Correction with External Attitude Measurements

As in section III, let the true attitude be represented by the rotation matrix, $\mathbf{C}_{bI}$, and the external attitude measurement and gyro-propagated attitude estimate be represented by the rotation matrices $\hat{\mathbf{C}}_{bI}^M$ and $\hat{\mathbf{C}}_{bi}^G$ respectively. The attitude

errors for the external attitude measurement and gyro attitude estimate are defined to be the rotation matrices

$$\delta\mathbf{C}^M = \hat{\mathbf{C}}_{bI}^M \mathbf{C}_{bI}^{-1} \quad \textbf{(10)}$$

and

$$\delta\mathbf{C}^G = \hat{\mathbf{C}}_{bI}^G \mathbf{C}_{bI}^{-1} \quad \textbf{(11)}$$

respectively. To correct the gyro attitude estimate, it is necessary to estimate $\delta\mathbf{C}^G$. As for the external attitude measurement error, the gyro attitude error, $\delta\mathbf{C}^G$, is parameterized by the quaternion, $(\boldsymbol{\varepsilon}, \eta)$. In this case, estimating $(\boldsymbol{\varepsilon}, \eta)$ is equivalent to estimating $\delta\mathbf{C}^G$. Post-multiplying the gyro attitude estimate (11) by the inverse of the external attitude measurement (10) leads to the measured gyro attitude estimate error, given by

$$\delta\mathbf{C}^{GM} := \hat{\mathbf{C}}_{bI}^G \left(\hat{\mathbf{C}}_{bI}^M\right)^{-1} = \delta\mathbf{C}^G \left(\delta\mathbf{C}^M\right)^{-1} = \delta\mathbf{C}^G \left(\delta\mathbf{C}^M\right)^T \quad \textbf{(12)}$$

Parameterizing $\delta\mathbf{C}^{GM}$ by the quaternion $(\boldsymbol{\varepsilon}_{GM}, \eta_{GM})$, as required later in the paper, the filter input will be computed as

$$\boldsymbol{y} = \boldsymbol{\varepsilon}_{GM}\, sign(\eta_{GM}), \quad \textbf{(13)}$$

where

$$sign(x) = \begin{cases} 1, & x \geq 0, \\ -1, & x < 0. \end{cases} \quad \textbf{(14)}$$

Note that in general the quaternion $(\boldsymbol{\varepsilon}, \eta)$ and $(-\boldsymbol{\varepsilon}, -\eta)$ represent the same attitude. Therefore the filter input in equation (13) is unambiguous, except when $\eta_{GM} = 0$, which means that care needs to be taken when this condition arises. Making use of the composition rules for quaternions [11], the filter input in equation (13) can be written as

$$\boldsymbol{y} = \left[\eta_M \boldsymbol{\varepsilon} - \eta \boldsymbol{v}_M + \boldsymbol{\varepsilon}^{\times} \boldsymbol{v}_M\right] sign\left(\eta_M \eta + \boldsymbol{\varepsilon}^T \boldsymbol{v}_M\right) \quad (15)$$

In the noise-free case, $(\boldsymbol{v}_M, \eta_M) = (\boldsymbol{0}, \pm 1)$, and the filter input in equation (13) becomes

$$\boldsymbol{y} = \boldsymbol{\varepsilon}\, sign(\eta). \quad (16)$$

Assume for the moment that

$$\boldsymbol{\varepsilon}^T \boldsymbol{\varepsilon} < 1 - \boldsymbol{v}_M^T \boldsymbol{v}_M . \quad (17)$$

By the Cauchy-Schwarz inequality, $\left(\boldsymbol{\varepsilon}^T \boldsymbol{v}_M\right)^2 \leq \boldsymbol{\varepsilon}^T \boldsymbol{\varepsilon} \boldsymbol{v}_M^T \boldsymbol{v}_M$. Combining this with (17) leads to $\left|\boldsymbol{\varepsilon}^T \boldsymbol{v}_M\right| < \left(1 - \boldsymbol{v}_M^T \boldsymbol{v}_M\right)^{\frac{1}{2}} \left(1 - \boldsymbol{\varepsilon}^T \boldsymbol{\varepsilon}\right)^{\frac{1}{2}} = \left|\eta_M \eta\right|$. This implies that

$$sign(\eta_M \eta + \boldsymbol{\varepsilon}^T \mathbf{v}_M) = sign(\eta_M \eta) = sign(\eta_M)\, sign(\eta). \quad \textbf{(18)}$$

Under the condition (18), with the further assumption that $\|\boldsymbol{v}_M\| << 1$, the filter input equation (15) becomes

$$\boldsymbol{y} = \boldsymbol{\varepsilon} sign(\eta) - \bar{\boldsymbol{\nu}}_M, \tag{19}$$

where $\bar{\boldsymbol{\nu}}_M = -sign(\eta_M)\boldsymbol{\nu}_M + sign(\eta)sign(\eta_M)\boldsymbol{\varepsilon}^{\times}\boldsymbol{\nu}_M$. Since $(\boldsymbol{\nu}_M, \eta_M)$ and $(-\boldsymbol{\nu}_M, -\eta_M)$ represent the same measurement error, $sign(\eta_M) = 1$ can be chosen. Finally, in the design of the Kalman filter, the case of small $\boldsymbol{\varepsilon}$ will be of interest as well, in which case the filter input (15) becomes

$$\boldsymbol{y} = \boldsymbol{\varepsilon} sign(\eta) - \boldsymbol{\nu}_M . \tag{20}$$

Two cases will be considered, denoted case (a) and case (b) respectively. In case (a), the measured angular velocity and correction are treated as vectors expressed in the estimated body frame. As will be shown, this leads to a simplified expression (compared to case (b)) of the appearance of measurement noise in the error dynamics, however, the error dynamics in this case explicitly contain a term depending on the angular velocity $\boldsymbol{\omega}$. This means that a given constant gain filter is not necessarily optimal for an arbitrary spacecraft angular motion. In case (b) on the other hand, the measured angular velocity and correction are treated as vectors expressed in the true body frame, and the error dynamics in this case are independent of the spacecraft angular velocity $\boldsymbol{\omega}$. This is very useful for the design of a Kalman filter, since the linearized dynamics are time-invariant, and the Kalman gain does not depend on the spacecraft angular motion. Now, all that is needed are the dynamical equations for $(\boldsymbol{\varepsilon}, \eta)$. With a view to applying gyro attitude estimate corrections, let the gyro estimates be obtained by integrating

$$\dot{\hat{\mathbf{C}}}_{bI}^{G} = -\bar{\boldsymbol{\omega}}^{\times}\hat{\mathbf{C}}_{bI}^{G} \text{ or } \dot{\hat{\boldsymbol{\alpha}}} = \mathbf{W}(\hat{\boldsymbol{\alpha}})\bar{\boldsymbol{\omega}}, \tag{21}$$

depending upon the attitude parameterization, where

$$\bar{\boldsymbol{\omega}} = \begin{cases} \boldsymbol{\omega}^m + \boldsymbol{u}, & case\ (a), \\ \hat{\mathbf{C}}_{bI}^{G}\left(\hat{\mathbf{C}}_{bI}^{M}\right)^{-1}\left(\boldsymbol{\omega}^m + \boldsymbol{u}\right), & case\ (b), \end{cases} \tag{22}$$

and $\boldsymbol{u}$ is a correction parameter to be determined. This correction parameter $\boldsymbol{u}$ is in keeping with the closed-loop filter implementation (see [1]). As shown in reference [1], closed-loop filter implementation is mathematically equivalent to open-loop implementation, and is desirable from a practical viewpoint since it is computationally simpler, more robust, and it keeps the gyro attitude estimate errors small.

Case (a)

Now, consider two reference frames, the true spacecraft body frame, $\Im_b$ (whose attitude is given by $\mathbf{C}_{bI}$), and the gyro estimate of the spacecraft body frame $\Im_b^G$ (whose attitude is given by $\hat{\mathbf{C}}_{bI}^{G}$). Clearly, as seen in (11), the gyro attitude error $\delta\mathbf{C}^G$ represents a rotation from the true body frame to the estimated body frame. From (21) and (22), it is seen that

the angular velocity of the estimated body frame (expressed in the estimated frame), is $\bar{\boldsymbol{\omega}} = \boldsymbol{\omega}^m + \boldsymbol{u}$. From equation (1), it is seen that the angular velocity of the true body frame (expressed in the true frame) is $\boldsymbol{\omega}$. Making use of equation (3) for the measured angular velocity leads to

$$\bar{\boldsymbol{\omega}} = \boldsymbol{\omega} + \boldsymbol{u} + \boldsymbol{b}_\omega + \boldsymbol{w}_\omega . \tag{23}$$

Now, the angular velocity of the estimated body frame *relative* to the true body frame (expressed in the estimated body frame) is

$$\begin{aligned} \delta\boldsymbol{\omega} &= \bar{\boldsymbol{\omega}} - \delta\mathbf{C}^G(\boldsymbol{\varepsilon},\eta)\boldsymbol{\omega} \\ &= \left(\mathbf{I} - \delta\mathbf{C}^G(\boldsymbol{\varepsilon},\eta)\right)\boldsymbol{\omega} + \boldsymbol{u} + \boldsymbol{b}_\omega + \boldsymbol{w}_\omega . \end{aligned} \tag{24}$$

With equation (24) in hand, the kinematical equations for $(\boldsymbol{\varepsilon},\eta)$ are given by [11]

$$\begin{aligned} \dot{\boldsymbol{\varepsilon}} &= \mathbf{S}(\boldsymbol{\varepsilon},\eta)\delta\boldsymbol{\omega}, \\ \dot{\eta} &= -\frac{\boldsymbol{\varepsilon}^T\delta\boldsymbol{\omega}}{2}, \end{aligned} \tag{25}$$

where

$$\mathbf{S}(\boldsymbol{\varepsilon},\eta) = \frac{1}{2}\left(\eta I + \boldsymbol{\varepsilon}^\times\right). \tag{26}$$

Therefore, the kinematics of the estimated body frame with respect to the true body frame are given by

$$\begin{aligned} \dot{\boldsymbol{\varepsilon}} &= \mathbf{S}(\boldsymbol{\varepsilon},\eta)\left(\mathbf{I} - \delta\mathbf{C}^G(\boldsymbol{\varepsilon},\eta)\right)\boldsymbol{\omega} + \mathbf{S}(\boldsymbol{\varepsilon},\eta)\boldsymbol{u} + \mathbf{S}(\boldsymbol{\varepsilon},\eta)\boldsymbol{b}_\omega + \mathbf{S}(\boldsymbol{\varepsilon},\eta)\boldsymbol{w}_\omega , \\ \dot{\eta} &= -\frac{1}{2}\boldsymbol{\varepsilon}^T\left(\boldsymbol{\omega} + \boldsymbol{u} - \delta\mathbf{C}^G(\boldsymbol{\varepsilon},\eta)\boldsymbol{\omega} + \boldsymbol{b}_\omega + \boldsymbol{w}_\omega\right). \end{aligned} \tag{27}$$

It can be readily shown that

$$\begin{aligned} \mathbf{S}(\boldsymbol{\varepsilon},\eta)\delta\mathbf{C}^G(\boldsymbol{\varepsilon},\eta) &= \mathbf{S}(-\boldsymbol{\varepsilon},\eta), \\ \boldsymbol{\varepsilon}^T\delta\mathbf{C}^G(\boldsymbol{\varepsilon},\eta) &= \boldsymbol{\varepsilon}^T. \end{aligned} \tag{28}$$

Together with the bias model (4), the full set of gyro attitude error equations become

$$\begin{aligned} \dot{\boldsymbol{\varepsilon}} &= -\boldsymbol{\omega}^\times\boldsymbol{\varepsilon} + \mathbf{S}(\boldsymbol{\varepsilon},\eta)\left(\boldsymbol{b}_\omega + \boldsymbol{u} + \boldsymbol{w}_\omega\right), \\ \dot{\eta} &= -\frac{1}{2}\boldsymbol{\varepsilon}^T\left(\boldsymbol{b}_\omega + \boldsymbol{u} + \boldsymbol{w}_\omega\right), \\ \dot{\boldsymbol{b}}_\omega &= \boldsymbol{w}_{b\omega}. \end{aligned} \tag{29}$$

In order to choose the control law, it is useful to examine the noise-free case $\boldsymbol{w}_\omega \equiv \boldsymbol{w}_{b\omega} \equiv \boldsymbol{v}_M = \boldsymbol{0}$. Defining the bias estimation error to be $\tilde{\boldsymbol{b}}_\omega = \boldsymbol{b}_\omega - \hat{\boldsymbol{b}}_\omega$, where $\hat{\boldsymbol{b}}_\omega$ is the bias estimate, a control and estimation law are sought such that $\boldsymbol{\varepsilon} \to \boldsymbol{0}$ and $\tilde{\boldsymbol{b}}_\omega \to \boldsymbol{0}$. To this end, choose

$$\begin{aligned}\boldsymbol{u} &= -\hat{\boldsymbol{b}}_\omega - \mathbf{K}_p \boldsymbol{\varepsilon} sign(\eta), \\ \dot{\hat{\boldsymbol{b}}}_\omega &= \mathbf{K}_b \boldsymbol{\varepsilon} sign(\eta),\end{aligned} \tag{30}$$

where $\mathbf{K}_p = \mathbf{K}_p^T > \mathbf{0}$ and $\mathbf{K}_b = \mathbf{K}_b^T > \mathbf{0}$ are positive definite matrices. Then, the closed-loop error dynamics become

$$\begin{aligned}\dot{\boldsymbol{\varepsilon}} &= -\boldsymbol{\omega}^\times \boldsymbol{\varepsilon} + \mathbf{S}(\boldsymbol{\varepsilon}, \eta)\left(\tilde{\boldsymbol{b}}_\omega - \mathbf{K}_p \boldsymbol{\varepsilon} sign(\eta)\right), \\ \dot{\eta} &= -\frac{1}{2}\boldsymbol{\varepsilon}^T\left(\tilde{\boldsymbol{b}}_\omega - \mathbf{K}_p \boldsymbol{\varepsilon} sign(\eta)\right), \\ \dot{\tilde{\boldsymbol{b}}}_\omega &= -\mathbf{K}_b \boldsymbol{\varepsilon} sign(\eta).\end{aligned} \tag{31}$$

Assumption 1: The angular rate $\boldsymbol{\omega}(t)$ is continuous in t and bounded

Theorem 1: Under Assumption 1, the closed-loop equations (31) are globally stable.

Proof: Contained in the appendix.

With a further restriction on $\mathbf{K}_p$, a stronger claim about the stability can be made.

Theorem 2: Under Assumption 1, the closed-loop equations (31) exhibit exponential convergence if in addition, $\mathbf{K}_p = k_p \mathbf{I}$ for some positive scalar k_p.

Proof: Contained in the appendix.

Case (b)

In this case, making use of (22) and (12), the angular velocity of the estimated body frame becomes

$$\bar{\boldsymbol{\omega}} = \delta\mathbf{C}^G(\boldsymbol{\varepsilon}, \eta)\left(\delta\mathbf{C}^M(\boldsymbol{v}_M, \eta_M)\right)^T\left(\boldsymbol{\omega}^m + \boldsymbol{u}\right). \tag{32}$$

Proceeding with the same derivation as for case (a), this leads to

$$\delta\boldsymbol{\omega} = \delta\mathbf{C}^G(\boldsymbol{\varepsilon}, \eta)\left(\left(\left(\delta\mathbf{C}^M(\boldsymbol{v}_M, \eta_M)\right)^T - I\right)\boldsymbol{\omega} + \left(\delta\mathbf{C}^M(\boldsymbol{v}_M, \eta_M)\right)^T\left(\boldsymbol{u} + \boldsymbol{b}_\omega + \boldsymbol{w}_\omega\right)\right). \tag{33}$$

Making the assumption that $\|\boldsymbol{v}_M\| << 1$ gives the approximation $\delta\mathbf{C}^M \approx I - 2\boldsymbol{v}_M^\times$, so that (33) can be written as

$$\delta\boldsymbol{\omega} = \delta\mathbf{C}^G(\boldsymbol{\varepsilon}, \eta)\left(\left(\boldsymbol{u} + \boldsymbol{b}_\omega + \boldsymbol{w}_\omega\right) + 2\boldsymbol{v}_M^\times\left(\boldsymbol{\omega} + \boldsymbol{u} + \boldsymbol{b}_\omega + \boldsymbol{w}_\omega\right)\right). \tag{34}$$

Making use of (25) and (28), leads to the dynamical equations for $(\boldsymbol{\varepsilon}, \eta)$ which are

$$\begin{aligned}\dot{\boldsymbol{\varepsilon}} &= \mathbf{S}(-\boldsymbol{\varepsilon}, \eta)\left(\left(\boldsymbol{u} + \boldsymbol{b}_\omega + \boldsymbol{w}_\omega\right) + 2\boldsymbol{v}_M^\times\left(\boldsymbol{\omega} + \boldsymbol{u} + \boldsymbol{b}_\omega + \boldsymbol{w}_\omega\right)\right), \\ \dot{\eta} &= -\frac{1}{2}\boldsymbol{\varepsilon}^T\left(\left(\boldsymbol{u} + \boldsymbol{b}_\omega + \boldsymbol{w}_\omega\right) + 2\boldsymbol{v}_M^\times\left(\boldsymbol{\omega} + \boldsymbol{u} + \boldsymbol{b}_\omega + \boldsymbol{w}_\omega\right)\right).\end{aligned} \tag{35}$$

As was mentioned before, in this case, the angular motion of the spacecraft is eliminated from the noise-free dynamics, but it has effectively increased the process noise by the additional term $\boldsymbol{\omega}^\times \boldsymbol{v}_M$, which could lead to deteriorated performance with increased measurement noise or angular velocity compared with the filter in case (a). This will be examined further in section V.

As for case (a), the noise-free case ($\boldsymbol{w}_{\omega} \equiv \boldsymbol{w}_{b\omega} \equiv \boldsymbol{v}_M = \boldsymbol{0}$) is considered, and the same control and estimation laws given by (30) are chosen. Then, the closed-loop error dynamics become

$$\begin{aligned} \dot{\boldsymbol{\varepsilon}} &= \mathbf{S}(-\boldsymbol{\varepsilon},\eta)\left(\tilde{\boldsymbol{b}}_{\omega} - \mathbf{K}_p \boldsymbol{\varepsilon} sign(\eta)\right), \\ \dot{\eta} &= -\frac{1}{2}\boldsymbol{\varepsilon}^T\left(\tilde{\boldsymbol{b}}_{\omega} - \mathbf{K}_p \boldsymbol{\varepsilon} sign(\eta)\right), \\ \dot{\tilde{\boldsymbol{b}}}_{\omega} &= -\mathbf{K}_b \boldsymbol{\varepsilon} sign(\eta). \end{aligned} \qquad (36)$$

As for case (a) the following results are obtained:

Theorem 3: Under Assumption 1, the closed-loop equations (36) are globally stable.

Proof: Contained in the appendix.

Theorem 4: Under Assumption 1, the closed-loop equations (36) exhibit exponential convergence if in addition, $\mathbf{K}_p = k_p \mathbf{I}$ for some positive scalar k_p.

Proof: Contained in the appendix.

Remark

Note that the observer of reference [5] is a special case of case (b) with $\mathbf{K}_p = k_p \mathbf{I}$ and $\mathbf{K}_b = \frac{1}{2}\mathbf{I}$, while representing the gyro propagated attitude $\hat{\mathbf{C}}_{bI}^{G}$ and the measured attitude $\hat{\mathbf{C}}_{bI}^{M}$ in terms of quaternions.

V. Filter Gain Selection and Steady-State Performance

A. Gain Selection

In reality, the noise free quaternion $(\boldsymbol{\varepsilon},\eta)$ is not available as a measurement. Instead, the filter input available is as defined in equation (13). Therefore, the control and estimation laws are obtained by substituting the measurement $\boldsymbol{y}$ for $\boldsymbol{\varepsilon} sign(\eta)$ to yield

$$\begin{aligned} \boldsymbol{u} &= -\hat{\boldsymbol{b}}_{\omega} - \mathbf{K}_p \boldsymbol{y}, \\ \dot{\hat{\boldsymbol{b}}}_{\omega} &= \mathbf{K}_b \boldsymbol{y}. \end{aligned} \qquad \textbf{(37)}$$

From theorems 1 and 3, choosing constant gains $\mathbf{K}_p > \mathbf{0}$ and $\mathbf{K}_b > \mathbf{0}$ renders the filter globally stable. It makes sense to choose the gains based upon the steady-state filter performance with respect to process and measurement noise. The process and measurement noise are taken to be zero-mean white noise processes with covariances $E\left\{\boldsymbol{w}\boldsymbol{w}^T\right\} = \mathbf{Q} \geq \mathbf{0}$ and $E\left\{\boldsymbol{v}_M \boldsymbol{v}_M^T\right\} = \mathbf{R} > \mathbf{0}$ respectively. Note that no assumption is being made on the type of distribution (it does not have to be Gaussian). This allows the assumption to be made that the measurement error $\boldsymbol{v}_M$ is small (unlike the Gaussian

distribution, which has infinite tails). Note that this means that the Kalman Filter is not necessarily the optimal filter, however it is the optimal linear filter [15].

Given that the attitude errors are expected to be small in steady-state, it is reasonable to choose the gains based upon the linearized system only. For small $\boldsymbol{\varepsilon}$, $|\eta| \approx 1$ and $sign(\eta)$ is constant. Therefore, the dynamics of η do not need to be considered. As noted in (20), the filter input becomes

$$\boldsymbol{y} = \boldsymbol{\varepsilon} sign(\eta) - \boldsymbol{v}_M, \quad E\left\{\boldsymbol{v}_M \boldsymbol{v}_M^T\right\} = \mathbf{R} > \mathbf{0}. \tag{38}$$

Reintroducing the system noise and performing the linearization of the error dynamics assuming that $sign(\eta) = 1$, the closed-loop system is

$$\begin{bmatrix} \dot{\boldsymbol{\varepsilon}} \\ \dot{\tilde{\boldsymbol{b}}}_\omega \end{bmatrix} = \begin{bmatrix} -\boldsymbol{\omega}^\times & \mathbf{0} \\ \mathbf{0} & \mathbf{0} \end{bmatrix} \begin{bmatrix} \boldsymbol{\varepsilon} \\ \tilde{\boldsymbol{b}}_\omega \end{bmatrix} + \begin{bmatrix} -\frac{\mathbf{K}_p}{2} & \frac{\mathbf{I}}{2} \\ -\mathbf{K}_b & \mathbf{0} \end{bmatrix} \begin{bmatrix} \boldsymbol{\varepsilon} \\ \tilde{\boldsymbol{b}}_\omega \end{bmatrix} - \begin{bmatrix} \frac{\mathbf{K}_p}{2} \\ \mathbf{K}_b \end{bmatrix} \boldsymbol{v}_M + \begin{bmatrix} \frac{\mathbf{I}}{2} & \mathbf{0} \\ \mathbf{0} & \mathbf{I} \end{bmatrix} \begin{bmatrix} \boldsymbol{w}_\omega \\ \boldsymbol{w}_{b\omega} \end{bmatrix}, \tag{39}$$

for case (a), and

$$\begin{bmatrix} \dot{\boldsymbol{\varepsilon}} \\ \dot{\tilde{\boldsymbol{b}}}_\omega \end{bmatrix} = \begin{bmatrix} -\frac{\mathbf{K}_p}{2} & \frac{\mathbf{I}}{2} \\ -\mathbf{K}_b & \mathbf{0} \end{bmatrix} \begin{bmatrix} \boldsymbol{\varepsilon} \\ \tilde{\boldsymbol{b}}_\omega \end{bmatrix} - \begin{bmatrix} \frac{\mathbf{K}_p}{2} \\ \mathbf{K}_b \end{bmatrix} \boldsymbol{v}_M + \begin{bmatrix} \frac{\mathbf{I}}{2} & \mathbf{0} \\ \mathbf{0} & \mathbf{I} \end{bmatrix} \begin{bmatrix} \boldsymbol{w}_\omega \\ \boldsymbol{w}_{b\omega} \end{bmatrix} - \begin{bmatrix} \boldsymbol{\omega}^\times \\ \mathbf{0} \end{bmatrix} \boldsymbol{v}_M, \tag{40}$$

for case (b). If $sign(\eta) = -1$, then the closed-loop system can be written in terms of the negative bias error $\tilde{\boldsymbol{b}}_{\omega n} := -\tilde{\boldsymbol{b}}_\omega$, in which case the linearized closed-loop equations become

$$\begin{bmatrix} \dot{\boldsymbol{\varepsilon}} \\ \dot{\tilde{\boldsymbol{b}}}_{n\omega} \end{bmatrix} = \begin{bmatrix} -\boldsymbol{\omega}^\times & \mathbf{0} \\ \mathbf{0} & \mathbf{0} \end{bmatrix} \begin{bmatrix} \boldsymbol{\varepsilon} \\ \tilde{\boldsymbol{b}}_{n\omega} \end{bmatrix} + \begin{bmatrix} -\frac{\mathbf{K}_p}{2} & \frac{\mathbf{I}}{2} \\ -\mathbf{K}_b & \mathbf{0} \end{bmatrix} \begin{bmatrix} \boldsymbol{\varepsilon} \\ \tilde{\boldsymbol{b}}_{n\omega} \end{bmatrix} - \begin{bmatrix} \frac{\mathbf{K}_p}{2} \\ \mathbf{K}_b \end{bmatrix} \boldsymbol{v}_M + \begin{bmatrix} \frac{\mathbf{I}}{2} & \mathbf{0} \\ \mathbf{0} & \mathbf{I} \end{bmatrix} \begin{bmatrix} \boldsymbol{w}_\omega \\ -\boldsymbol{w}_{b\omega} \end{bmatrix}, \tag{41}$$

for case (a), and

$$\begin{bmatrix} \dot{\boldsymbol{\varepsilon}} \\ \dot{\tilde{\boldsymbol{b}}}_{n\omega} \end{bmatrix} = \begin{bmatrix} -\frac{\mathbf{K}_p}{2} & \frac{\mathbf{I}}{2} \\ -\mathbf{K}_b & \mathbf{0} \end{bmatrix} \begin{bmatrix} \boldsymbol{\varepsilon} \\ \tilde{\boldsymbol{b}}_{n\omega} \end{bmatrix} - \begin{bmatrix} \frac{\mathbf{K}_p}{2} \\ \mathbf{K}_b \end{bmatrix} \boldsymbol{v}_M + \begin{bmatrix} \frac{\mathbf{I}}{2} & \mathbf{0} \\ \mathbf{0} & \mathbf{I} \end{bmatrix} \begin{bmatrix} \boldsymbol{w}_\omega \\ -\boldsymbol{w}_{b\omega} \end{bmatrix} - \begin{bmatrix} \boldsymbol{\omega}^\times \\ \mathbf{0} \end{bmatrix} \boldsymbol{v}_M, \tag{42}$$

for case (b). Comparing equations (39) and (40) with (41) and (42) respectively, it can that the steady-state behavior will be the same regardless of the sign of η. As can be seen in equations (40) and (42), the process noise has been increased by the term $\boldsymbol{\omega}^\times \boldsymbol{v}_M$ in case (b).

Since the gains are to be the same regardless of the angular velocities (they are constant), they will be chosen for the case of zero angular velocity ($\boldsymbol{\omega} \equiv \boldsymbol{0}$). The steady-state performance using those gains with non-zero angular velocity will then be compared with the steady-state performance with zero angular velocity. Setting $\boldsymbol{\omega} \equiv \boldsymbol{0}$, for both cases (a) and (b) the gain selection is based upon the system

$$\begin{bmatrix} \dot{\boldsymbol{\varepsilon}} \\ \dot{\tilde{\boldsymbol{b}}}_{n\omega} \end{bmatrix} = \begin{bmatrix} -\dfrac{\mathbf{K}_p}{2} & \dfrac{\mathbf{I}}{2} \\ -\mathbf{K}_b & \mathbf{0} \end{bmatrix} \begin{bmatrix} \boldsymbol{\varepsilon} \\ \tilde{\boldsymbol{b}}_{n\omega} \end{bmatrix} - \begin{bmatrix} \dfrac{\mathbf{K}_p}{2} \\ \mathbf{K}_b \end{bmatrix} \boldsymbol{v}_p + \begin{bmatrix} \dfrac{\mathbf{I}}{2} & \mathbf{0} \\ \mathbf{0} & \mathbf{I} \end{bmatrix} \begin{bmatrix} \boldsymbol{w}_\omega \\ \boldsymbol{w}_{b\omega} \end{bmatrix}. \tag{43}$$

The linear optimal gains may now be obtained from the Kalman filter corresponding to this system. It is useful to define the following matrices and vectors

$$\begin{aligned} &\mathbf{A} = \begin{bmatrix} \mathbf{0} & \dfrac{\mathbf{I}}{2} \\ \mathbf{0} & \mathbf{0} \end{bmatrix}, \quad \mathbf{K} = \begin{bmatrix} \bar{\mathbf{K}}_p \\ \mathbf{K}_b \end{bmatrix}, \quad \bar{\mathbf{K}}_p = \frac{\mathbf{K}_p}{2}, \quad \mathbf{H} = \begin{bmatrix} \mathbf{I} & \mathbf{0} \end{bmatrix}, \mathbf{G} = \begin{bmatrix} \dfrac{\mathbf{I}}{2} & \mathbf{0} \\ \mathbf{0} & \mathbf{I} \end{bmatrix}, \\ &\boldsymbol{x} = \begin{bmatrix} \boldsymbol{\varepsilon} \\ \tilde{\boldsymbol{b}}_\omega \end{bmatrix}, \boldsymbol{w} = \begin{bmatrix} \boldsymbol{w}_\omega \\ \boldsymbol{w}_{b\omega} \end{bmatrix}, \mathbf{P} = E\left\{ \boldsymbol{x}\boldsymbol{x}^T \right\} \text{ and } \mathbf{Q} = E\left\{ \boldsymbol{w}\boldsymbol{w}^T \right\} \end{aligned} \quad . \tag{44}$$

With these definitions, the closed-loop gyro error equations are given by

$$\dot{\boldsymbol{x}} = \left(\mathbf{A} - \mathbf{KH} \right) \boldsymbol{x} - \mathbf{K}\boldsymbol{v}_M + \mathbf{G}\boldsymbol{w}$$

Then, the evolution of the state error covariance is described by (see [15])

$$\dot{\mathbf{P}} = \left(\mathbf{A} - \mathbf{KH} \right) \mathbf{P} + \mathbf{P} \left(\mathbf{A} - \mathbf{KH} \right)^T + \mathbf{KRK}^T + \mathbf{GQG}^T, \tag{45}$$

and in anticipation of $\left(\mathbf{A} - \mathbf{KH} \right)$ being stable, this converges to a constant steady-state matrix, satisfying

$$\left(\mathbf{A} - \mathbf{KH} \right) \mathbf{P}_{ss} + \mathbf{P}_{ss} \left(\mathbf{A} - \mathbf{KH} \right)^T + \mathbf{KRK}^T + \mathbf{GQG}^T = \mathbf{0}. \tag{46}$$

The gain $\mathbf{K}$ is chosen to minimize the cost function $J = trace\left\{ \mathbf{P}_{ss} \right\}$. To simplify the analysis, $\mathbf{Q}$ and $\mathbf{R}$ are assumed to have the form

$$\mathbf{R} = r\mathbf{I}, \quad \mathbf{Q} = \begin{bmatrix} q_p \mathbf{I} & 0 \\ 0 & q_b \mathbf{I} \end{bmatrix}. \tag{47}$$

Remark

In practice, the measurement and process noise covariances are not constant and isotropic as in (47). However, if $\mathbf{Q}$ and $\mathbf{R}$ are chosen so that $\mathbf{Q}_T(t) \le \mathbf{Q}$ and $\mathbf{R}_T(t) \le \mathbf{R}$ where $\mathbf{Q}_T(t)$ and $\mathbf{R}_T(t)$ are the true process and measurement noise covariances, then the true state error covariance $\mathbf{P}_T(t) = E\left\{ \boldsymbol{x}(t)\boldsymbol{x}^T(t) \right\}$ satisfies $\mathbf{P}_T(t) \le \mathbf{P}(t)$ for all time $t \ge 0$. This can be easily shown as follows. The true state error covariance satisfies $\dot{\mathbf{P}}_T = \left(\mathbf{A} - \mathbf{KH} \right) \mathbf{P}_T + \mathbf{P}_T \left(\mathbf{A} - \mathbf{KH} \right)^T + \mathbf{KR}_T\mathbf{K}^T + \mathbf{GQ}_T\mathbf{G}^T$. Defining the difference $\tilde{\mathbf{P}}(t) = \mathbf{P}(t) - \mathbf{P}_T(t)$, leads to $\dot{\tilde{\mathbf{P}}} = \left(\mathbf{A} - \mathbf{KH} \right) \tilde{\mathbf{P}} + \tilde{\mathbf{P}} \left(\mathbf{A} - \mathbf{KH} \right)^T + \mathbf{K} \left(\mathbf{R} - \mathbf{R}_T \right) \mathbf{K}^T + \mathbf{G} \left(\mathbf{Q} - \mathbf{Q}_T \right) \mathbf{G}^T$. Taking $\mathbf{P}(0) = \mathbf{P}_T(0)$ leads to the solution $\tilde{\mathbf{P}}(t) = \int_0^t \boldsymbol{\Phi}(t,\tau) \left[\mathbf{K} \left(\mathbf{R} - \mathbf{R}_T \right) \mathbf{K}^T + \mathbf{G} \left(\mathbf{Q} - \mathbf{Q}_T \right) \mathbf{G}^T \right] \boldsymbol{\Phi}^T(t,\tau) d\tau \ge \mathbf{0}$, where $\boldsymbol{\Phi}(t,\tau)$ is the state-transition matrix corresponding to $\mathbf{A} - \mathbf{KH}$. Therefore, any bound on $\mathbf{P}(t)$ is automatically a bound on $\mathbf{P}_T(t)$. Note

that while this is shown here for the case of zero angular velocity, it can easily be shown to be true in both cases (a) and (b) for non-zero angular velocity.

Under the assumption (47), each channel decouples, and the steady-state Kalman gain matrix is given by (see [16])

$$\mathbf{K}_{Kalman} = \begin{bmatrix} \bar{k}_p \mathbf{I} \\ k_b \mathbf{I} \end{bmatrix}, \tag{48}$$

where

$$\begin{bmatrix} \bar{k}_p \\ k_b \end{bmatrix} = \begin{bmatrix} \frac{p_{11}}{r} \\ \frac{p_{12}}{r} \end{bmatrix}, \quad \begin{bmatrix} p_{11} & p_{12} \\ p_{12} & p_{22} \end{bmatrix} = \bar{\mathbf{P}}, \tag{49}$$

and $\bar{\mathbf{P}} > \mathbf{0}$ is the steady-state error variance for each channel, and satisfies

$$\bar{\mathbf{A}}\bar{\mathbf{P}} + \bar{\mathbf{P}}\bar{\mathbf{A}} - \frac{\bar{\mathbf{P}}\bar{\mathbf{H}}^{\mathrm{T}}\bar{\mathbf{H}}\bar{\mathbf{P}}}{r} + \bar{\mathbf{G}}\bar{\mathbf{Q}}\bar{\mathbf{G}}^{\mathrm{T}} = \mathbf{0}, \tag{50}$$

with the individual channel matrix definitions given by

$$\bar{\mathbf{A}} = \begin{bmatrix} 0 & \frac{1}{2} \\ 0 & 0 \end{bmatrix}, \quad \bar{\mathbf{H}} = \begin{bmatrix} 1 & 0 \end{bmatrix}, \quad \bar{\mathbf{G}} = \begin{bmatrix} \frac{1}{2} & 0 \\ 0 & 1 \end{bmatrix} \text{ and } \bar{\mathbf{Q}} = \begin{bmatrix} q_p & 0 \\ 0 & q_b \end{bmatrix}. \tag{51}$$

To show that the resulting steady-state Kalman gain is globally stabilizing, it suffices to show that $\bar{k}_p > 0$ and $k_b > 0$. Since the Kalman gain is locally stabilizing [16], the matrix

$$\begin{bmatrix} -\bar{k}_p & \frac{1}{2} \\ -k_b & 0 \end{bmatrix} \tag{52}$$

is stable. This has the characteristic equation

$$\lambda^2 + \bar{k}_p \lambda + \frac{k_b}{2} = 0, \tag{53}$$

which can only be asymptotically stable if $\bar{k}_p, k_b > 0$. Therefore, the steady-state Kalman gains are positive. This leads to the conclusion from Theorems 2 and 4 that the steady-state Kalman filter corresponding to (46), with gains obtained from (48)-(50), is globally stabilizing with exponential convergence when implemented in closed-loop form using equations (21), (22) and

$$\begin{aligned} \boldsymbol{u} &= -\hat{\boldsymbol{b}}_{\omega} - k_p \boldsymbol{\varepsilon} sign(\eta), \\ \dot{\hat{\boldsymbol{b}}}_{\omega} &= k_b \boldsymbol{\varepsilon} sign(\eta), \\ k_p &= 2\bar{k}_p. \end{aligned} \tag{54}$$

Summary of the Filter Algorithm

1. The external attitude measurement available is given by $\hat{\mathbf{C}}_{bI}^{M}$.
2. The gyro attitude estimate is given by the rotation matrix $\hat{\mathbf{C}}_{bi}^{G}$ or some other vector parameterization $\hat{\boldsymbol{\alpha}}$.
3. The measured gyro attitude error matrix is given by $\delta\mathbf{C}^{GM} = \hat{\mathbf{C}}_{bI}^{G}(\hat{\boldsymbol{\alpha}})\left(\hat{\mathbf{C}}_{bI}^{M}\right)^{-1}$.
4. The filter input is computed as $\boldsymbol{y} = \boldsymbol{\varepsilon}_{GM}\, sign(\eta_{GM})$, where $(\boldsymbol{\varepsilon}_{GM}, \eta_{GM})$ is the quaternion parameterization (see [11]) of the matrix $\delta\mathbf{C}^{GM}$.
5. The gyro attitude estimate is obtained by integrating the equations

$$\dot{\hat{\mathbf{C}}}_{bI}^{G} = -\bar{\boldsymbol{\omega}}^{\times}\hat{\mathbf{C}}_{bI}^{G} \quad \textbf{or} \quad \dot{\hat{\boldsymbol{\alpha}}} = \mathbf{W}(\hat{\boldsymbol{\alpha}})\bar{\boldsymbol{\omega}},$$

together with

$$\dot{\hat{\boldsymbol{b}}}_{\omega} = k_b \boldsymbol{y},$$

where

$$\bar{\boldsymbol{\omega}} = \begin{cases} \boldsymbol{\omega}^m - \hat{\boldsymbol{b}}_{\omega} - k_p \boldsymbol{y}, & case\ \ (a), \\ \delta\mathbf{C}^{GM}\left(\boldsymbol{\omega}^m - \hat{\boldsymbol{b}}_{\omega} - k_p \boldsymbol{y}\right), & case\ \ (b). \end{cases}$$

B. Steady-State Performance (Sub-Optimality of Filter)

The (linear) constant-gain filters presented in this paper are clearly sub-optimal. At steady-state (with small errors), the linear optimal filter is the Kalman Filter with in general time-varying gain, which depends upon the angular velocity [15]. It is difficult to determine how sub-optimal the filter is without knowing the angular velocity a-priori. Instead, the steady-state performance (for non-zero angular velocity) of the filters in cases (a) and (b) (using the scalar gains designed for zero angular velocity as in section V.A) are compared with the linear-optimal filter for the case of zero angular velocity. This is the subject of this section.

The action of the angular velocity in the error equations (39) and (41) for case (a) serves only to rotate the gyro error $\boldsymbol{\varepsilon}$, but does not change its magnitude ($\boldsymbol{\omega}^{\times}\boldsymbol{\varepsilon} \perp \boldsymbol{\varepsilon}$). Thus, it can be expected that similar performance will be achieved even when the angular velocity is significant. For the implementation of case (b), this is not the case, and the performance can be expected to deteriorate due to the effective increase in process noise as shown in equations (40) and (42). Finally, comparing equations (29) and (35), it would seem that the performance in case (b) is more sensitive to measurement noise than it is in case (a) even when the angular velocity is not significant.

In many cases, the angular velocity is approximately constant (for example spin-stabilized, earth pointing, sun pointing, etc.), so the case of constant angular velocity is considered first. With constant angular velocity, the closed-loop error

equations ((39)-(42)) are time-invariant. The result of this is that the steady-state error covariance is constant. In case (a), the steady-state error covariance satisfies

$$\left(\bar{\mathbf{A}}\text{-}\mathbf{KH}\right)\mathbf{P}_{ss,a}+\mathbf{P}_{ss,a}\left(\bar{\mathbf{A}}\text{-}\mathbf{KH}\right)^{T}+\mathbf{KRK}^{T}+\mathbf{GQG}^{T}=\mathbf{0}, \tag{55}$$

where

$$\bar{\mathbf{A}}=\begin{bmatrix}-\boldsymbol{\omega}^{\times} & \frac{\mathbf{I}}{2}\\ \mathbf{0} & \mathbf{0}\end{bmatrix},\ \mathbf{K}=\begin{bmatrix}\frac{k_p}{2}\mathbf{I}\\ k_b\mathbf{I}\end{bmatrix},\mathbf{P}_{ss,a}=\begin{bmatrix}\mathbf{P}_{\varepsilon\varepsilon ss,a} & \mathbf{P}_{\varepsilon bss,a}\\ \mathbf{P}_{\varepsilon bss,a}^{T} & \mathbf{P}_{bbss,a}\end{bmatrix},$$

$$\mathbf{P}_{\varepsilon\varepsilon ss,a}=\lim_{t\to\infty}E\left\{\boldsymbol{\varepsilon}\boldsymbol{\varepsilon}^{T}\right\},\mathbf{P}_{bbss,a}=\lim_{t\to\infty}E\left\{\tilde{\boldsymbol{b}}_{\omega}\tilde{\boldsymbol{b}}_{\omega}^{T}\right\},\mathbf{P}_{\varepsilon bss,a}=\lim_{t\to\infty}E\left\{\boldsymbol{\varepsilon}\tilde{\boldsymbol{b}}_{\omega}^{T}\right\}.$$

The solution of (55) can be obtained after some algebra and is given by

$$\begin{aligned}\mathbf{P}_{\varepsilon\varepsilon ss,a}&=\left(\frac{rk_b}{2k_p}+\frac{q_b}{2k_pk_b}+\frac{rk_p}{4}+\frac{q_p}{4k_p}\right)\mathbf{I},\\ \mathbf{P}_{bbss,a}&=\left(\frac{rk_b^2}{k_p}+\frac{q_b}{k_p}+\frac{q_bk_p}{2k_b}+\frac{q_pk_b}{2k_p}\right)\mathbf{I}+2\left(\frac{rk_b}{k_p}+\frac{q_b}{k_pk_b}\right)\left\|\boldsymbol{\omega}\right\|^{2}\mathbf{I}-2\left(\frac{rk_b}{k_p}+\frac{q_b}{k_pk_b}\right)\boldsymbol{\omega}\boldsymbol{\omega}^{T},\\ \mathbf{P}_{\varepsilon bss,a}&=\left(rk_b+\frac{q_b}{k_b}\right)\left(\frac{\mathbf{I}}{2}-\boldsymbol{\omega}^{\times}\right).\end{aligned} \tag{56}$$

Setting $\boldsymbol{\omega}=\boldsymbol{0}$ in (56) gives the steady-state error covariance in the case of zero angular velocity. From equation (56) it can be seen that for constant angular velocity, $\mathbf{P}_{\varepsilon\varepsilon ss,a}$ is independent of the angular velocity, and is the same as that for zero angular velocity. The only detrimental effect of the angular velocity is to increase the steady-state error covariance $\mathbf{P}_{bbss,a}$ by a factor that is proportional to the square of the angular velocity.

In case (b), the steady-state error covariance satisfies

$$\left(\mathbf{A}\text{-}\mathbf{KH}\right)\mathbf{P}_{ss,b}+\mathbf{P}_{ss,b}\left(\mathbf{A}\text{-}\mathbf{KH}\right)^{T}+\bar{\mathbf{K}}\mathbf{R}\bar{\mathbf{K}}^{T}+\mathbf{GQG}^{T}=\mathbf{0}, \tag{57}$$

where

$$\bar{\mathbf{K}}=\begin{bmatrix}\frac{k_p}{2}\mathbf{I}+\boldsymbol{\omega}^{\times}\\ k_b\mathbf{I}\end{bmatrix},\mathbf{P}_{ss,b}=\begin{bmatrix}\mathbf{P}_{\varepsilon\varepsilon ss,b} & \mathbf{P}_{\varepsilon bss,b}\\ \mathbf{P}_{\varepsilon bss,b}^{T} & \mathbf{P}_{bbss,b}\end{bmatrix},$$

$$\mathbf{P}_{\varepsilon\varepsilon ss,b}=\lim_{t\to\infty}E\left\{\boldsymbol{\varepsilon}\boldsymbol{\varepsilon}^{T}\right\},\mathbf{P}_{bbss,b}=\lim_{t\to\infty}E\left\{\tilde{\boldsymbol{b}}_{\omega}\tilde{\boldsymbol{b}}_{\omega}^{T}\right\},\mathbf{P}_{\varepsilon bss,b}=\lim_{t\to\infty}E\left\{\boldsymbol{\varepsilon}\tilde{\boldsymbol{b}}_{\omega}^{T}\right\}.$$

The solution of (57) can be obtained after some algebra, and is given by

$$\mathbf{P}_{\varepsilon\varepsilon ss,b}=\left(\frac{rk_b}{2k_p}+\frac{q_b}{2k_pk_b}+\frac{rk_p}{4}+\frac{q_p}{4k_p}\right)\mathbf{I}+\frac{r}{k_p}\|\boldsymbol{\omega}\|^2\mathbf{I}-\frac{r}{k_p}\boldsymbol{\omega}\boldsymbol{\omega}^T,$$
$$\mathbf{P}_{bbss,b}=\left(\frac{rk_b^2}{k_p}+\frac{q_b}{k_p}+\frac{q_bk_p}{2k_b}+\frac{q_pk_b}{2k_p}\right)\mathbf{I}+2\frac{rk_b}{k_p}\|\boldsymbol{\omega}\|^2\mathbf{I}-2\frac{rk_b}{k_p}\boldsymbol{\omega}\boldsymbol{\omega}^T, \quad (58)$$
$$\mathbf{P}_{\varepsilon bss,b}=\left(\frac{rk_b}{2}+\frac{q_b}{2k_b}\right)\mathbf{I}+2\frac{rk_b}{k_p}\boldsymbol{\omega}^{\times}.$$

It can be seen from equation (58) that unlike case (a), the angular velocity has detrimental effects on both $\mathbf{P}_{\varepsilon\varepsilon ss,b}$ and $\mathbf{P}_{bbss,b}$, increasing them both by factors proportional to the square of the angular velocity.

Next, the case of time-varying angular velocity is examined. Since the closed-loop system matrix ($\mathbf{A}$ - $\mathbf{KH}$) is constant in case (b), it is possible to obtain tight steady-state upper bounds on $\mathbf{P}_{\varepsilon\varepsilon,b}$ and $\mathbf{P}_{bb,b}$. Let $\mathbf{P}_b(t)=\begin{bmatrix}\mathbf{P}_{\varepsilon\varepsilon,b}(t) & \mathbf{P}_{\varepsilon b,b}(t)\\ \mathbf{P}_{\varepsilon b,b}^T(t) & \mathbf{P}_{bb,b}(t)\end{bmatrix}$ be the error covariance matrix for case (b) with arbitrary but bounded angular velocity $\|\boldsymbol{\omega}(t)\|\le\bar{\omega}$ for some $\bar{\omega}\ge 0$. This satisfies

$$\dot{\mathbf{P}}_b=(\mathbf{A}-\mathbf{KH})\mathbf{P}_b+\mathbf{P}_b(\mathbf{A}-\mathbf{KH})^T+(\mathbf{K}+\Delta\mathbf{K})\mathbf{R}(\mathbf{K}+\Delta\mathbf{K})^T+\mathbf{GQG}^T, \quad (59)$$

where $\Delta\mathbf{K}=\begin{bmatrix}\boldsymbol{\omega}^{\times}\\ \mathbf{0}\end{bmatrix}$. The difference with the steady-state error covariance for the zero angular velocity case is defined as $\tilde{\mathbf{P}}_b(t)=\mathbf{P}_b-\mathbf{P}_{ss}$, where $\mathbf{P}_{ss}$ satisfies (46). Subtracting (46) from (59) gives

$$\dot{\tilde{\mathbf{P}}}_b=(\mathbf{A}-\mathbf{KH})\tilde{\mathbf{P}}_b+\tilde{\mathbf{P}}_b(\mathbf{A}-\mathbf{KH})^T+\Delta\mathbf{KRK}^T+\mathbf{KR}\Delta\mathbf{K}^T+\Delta\mathbf{KR}\Delta\mathbf{K}^T. \quad (60)$$

This has the solution

$$\tilde{\mathbf{P}}_b(t)=\boldsymbol{\Phi}_b(t,0)\tilde{\mathbf{P}}_b(0)\boldsymbol{\Phi}_b^T(t,0)+\int_0^t\boldsymbol{\Phi}_b(t,\tau)\left[\Delta\mathbf{KRK}^T+\mathbf{KR}\Delta\mathbf{K}^T+\Delta\mathbf{KR}\Delta\mathbf{K}^T\right]\boldsymbol{\Phi}_b^T(t,\tau)d\tau, \quad (61)$$

where $\boldsymbol{\Phi}_b(t,\tau)$ is the state-transition matrix corresponding to $\mathbf{A}$ - $\mathbf{KH}$. Since only the steady-state part of $\tilde{\mathbf{P}}_b(t)$ is of interest, $\tilde{\mathbf{P}}_b(0)=\mathbf{0}$ is set. The state-transition matrix corresponding to $\mathbf{A}$ - $\mathbf{KH}$ can be shown to have the form

$$\boldsymbol{\Phi}_b(t,\tau)=\begin{bmatrix}\phi_{\varepsilon\varepsilon}(t,\tau)\mathbf{I} & \phi_{\varepsilon b}(t,\tau)\mathbf{I}\\ \phi_{b\varepsilon}(t,\tau)\mathbf{I} & \phi_{bb}(t,\tau)\mathbf{I}\end{bmatrix} \quad (62)$$

Substituting this into (61) with $\tilde{\mathbf{P}}_b(0)=\mathbf{0}$ and taking bounds on both sides leads to

$$\begin{aligned}\left\|\tilde{\mathbf{P}}_{\varepsilon\varepsilon,b}(t)\right\|_F &\le r\int_0^t\phi_{\varepsilon\varepsilon}^2(t,\tau)\left\|\boldsymbol{\omega}^{\times}\boldsymbol{\omega}^{\times}\right\|_F d\tau\le\sqrt{2}r\bar{\omega}^2\int_0^t\phi_{\varepsilon\varepsilon}^2(t,\tau)d\tau,\\ \left\|\tilde{\mathbf{P}}_{bb,b}(t)\right\|_F &\le r\int_0^t\phi_{b\varepsilon}^2(t,\tau)\left\|\boldsymbol{\omega}^{\times}\boldsymbol{\omega}^{\times}\right\|_F d\tau\le\sqrt{2}r\bar{\omega}^2\int_0^t\phi_{b\varepsilon}^2(t,\tau)d\tau,\end{aligned} \quad (63)$$

where $\|X\|_F = \sqrt{trace(XX^T)}$ is the Frobenius norm, and the identity $\left\|\boldsymbol{\omega}^{\times}\boldsymbol{\omega}^{\times}\right\|_F = \sqrt{2}\|\boldsymbol{\omega}\|_2^2$ has been used. The usefulness of the Frobenius norm is that for the *ii*th term $\{\mathbf{P}_b\}_{ii} = \{\mathbf{P}_{ss}\}_{ii} + \{\tilde{\mathbf{P}}_b\}_{ii} \le \{\mathbf{P}_{ss}\}_{ii} + \left|\{\tilde{\mathbf{P}}_b\}_{ii}\right| \le \{\mathbf{P}_{ss}\}_{ii} + \|\tilde{\mathbf{P}}_b\|_F$.

The relevant terms of the state transition matrix (62) can be found after some effort as

$$\phi_{\varepsilon\varepsilon}(t,\tau) = \begin{cases} e^{-\frac{k_p}{4}(t-\tau)}\left[\cos\left(\omega_d(t-\tau)\right) - \dfrac{k_p}{4\omega_d}\sin\left(\omega_d(t-\tau)\right)\right], & 8k_b > k_p^2, \\ e^{-\frac{k_p}{4}(t-\tau)} - \dfrac{k_p}{4}te^{-\frac{k_p}{4}(t-\tau)}, & 8k_b = k_p^2, \\ \dfrac{2}{\sqrt{k_p^2 - 8k_b}}\left[\lambda_{\max}e^{-\lambda_{\max}(t-\tau)} - \lambda_{\min}e^{-\lambda_{\min}(t-\tau)}\right], & 8k_b < k_p^2, \end{cases}$$

$$\phi_{b\varepsilon}(t,\tau) = \begin{cases} -\dfrac{k_b}{\omega_d}e^{-\frac{k_p}{4}(t-\tau)}\sin\left(\omega_d(t-\tau)\right), & 8k_b > k_p^2, \\ -k_b te^{-\frac{k_p}{4}(t-\tau)}, & 8k_b = k_p^2, \\ \dfrac{2k_b}{\sqrt{k_p^2 - 8k_b}}\left[e^{-\lambda_{\max}(t-\tau)} - e^{-\lambda_{\min}(t-\tau)}\right], & 8k_b < k_p^2, \end{cases} \quad \textbf{(64)}$$

where $\omega_d = \dfrac{\sqrt{8k_b - k_p^2}}{4}$ if $8k_b > k_p^2$, and $\lambda_{\min} = \dfrac{k_p - \sqrt{k_p^2 - 8k_b}}{4}, \lambda_{\max} = \dfrac{k_p + \sqrt{k_p^2 - 8k_b}}{4}$ if $8k_b < k_p^2$. By using the expressions in (64), it can be shown that

$$\int_0^t \phi_{\varepsilon\varepsilon}^2(t,\tau)d\tau \le \frac{1}{k_p}, \qquad \int_0^t \phi_{b\varepsilon}^2(t,\tau)d\tau \le \frac{2k_b}{k_p}. \quad \textbf{(65)}$$

Substituting these into (63) leads to the bounds

$$\left\|\tilde{\mathbf{P}}_{\varepsilon\varepsilon,b}(t)\right\|_F \le \frac{\sqrt{2}r\bar{\omega}^2}{k_p}, \qquad \left\|\tilde{\mathbf{P}}_{bb,b}(t)\right\|_F \le \frac{2\sqrt{2}rk_b\bar{\omega}^2}{k_p}. \quad (66)$$

It is interesting to examine the expressions for the steady-state values of $\tilde{\mathbf{P}}_{\varepsilon\varepsilon,b}$ and $\tilde{\mathbf{P}}_{bb,b}$ when the angular velocity is constant, can be obtained from (58) as

$$\lim_{t\to\infty}\tilde{\mathbf{P}}_{\varepsilon\varepsilon,b}(t)=\frac{r}{k_p}\boldsymbol{\omega}^{\times}\boldsymbol{\omega}^{\times},$$
$$\lim_{t\to\infty}\tilde{\mathbf{P}}_{bb,b}(t)=2\frac{rk_b}{k_p}\boldsymbol{\omega}^{\times}\boldsymbol{\omega}^{\times}. \qquad (67)$$

Taking the Frobenius norms of (67) gives

$$\lim_{t\to\infty}\left\|\tilde{\mathbf{P}}_{\varepsilon\varepsilon,b}(t)\right\|_F=\frac{\sqrt{2}r\left\|\boldsymbol{\omega}\right\|_2^2}{k_p},$$
$$\lim_{t\to\infty}\left\|\tilde{\mathbf{P}}_{bb,b}(t)\right\|_F=\frac{2\sqrt{2}rk_b\left\|\boldsymbol{\omega}\right\|_2^2}{k_p}, \qquad (68)$$

when the angular velocity is constant. Therefore, the upper bounds in (66) for arbitrary bounded time-varying angular velocities are in fact least upper bounds.

Unfortunately, it is not possible to obtain similar least upper bounds for case (a) for arbitrary bounded time-varying angular velocity without knowing the state-transition matrix corresponding to $\bar{\mathbf{A}}-\mathbf{KH}$. At least it is demonstrated by (56) and (58) that when the angular velocity is constant, the filter implementation of case (a) outperforms the implementation of case (b) in terms of steady-state performance. It will be demonstrated by a numerical example in the next section that the filter implementation of case (a) still outperforms the filter implementation of case (b) when the angular velocity is not constant.

VI. Numerical Example

In this section, the results in this paper are demonstrated, for the case of a satellite tumbling with an initial rate of 10 deg/s respectively. The satellite attitude motion is influenced by gravity-gradient and geomagnetic torque due to a residual magnetic dipole moment. The simulations are performed in MATLAB™. The initial uncertainties in the attitude and the gyro bias are taken to be

$$\sigma_1=\sigma_2=\left(\frac{\pi}{180}\right)^2.$$

The gyro provides measurements of the angular velocity given by

$$\boldsymbol{\omega}^m=\boldsymbol{\omega}+\boldsymbol{b}+\boldsymbol{w}_\omega, \qquad (69)$$

at a rate of 100 Hz, where each entry in $\mathbf{w}_\omega$ is a uniformly-distributed random number between the values of $\pm 0.05\ ^\circ/s$. The gyro bias is taken to be the constant

$$\boldsymbol{b} = \begin{bmatrix} 1 \\ -1 \\ 1 \end{bmatrix} \ ^\circ / s \qquad \textbf{(70)}$$

The external attitude measurements are available at a rate of 1 Hz, and are given by (5) with measurement error

$$\delta \mathbf{C}^M = \mathbf{I} + 2\left(\boldsymbol{v}_k^\times \boldsymbol{v}_k^\times - \left(1 - \boldsymbol{v}_k^T \boldsymbol{v}_k\right)^{\frac{1}{2}} \boldsymbol{v}_k^\times \right), \qquad \textbf{(71)}$$

where $\boldsymbol{v}_k$ is white zero-mean Gaussian noise sequence, with variance $E\left\{\boldsymbol{v}_k \boldsymbol{v}_k^T\right\} = r_d \mathbf{I}$, and $r_d = \left(\frac{\pi}{180}\right)^2$. The system and measurement noise covariances are taken to be

$$\mathbf{R} = r_d \Delta T \mathbf{I}, \quad \mathbf{Q} = \begin{bmatrix} \left(\frac{0.05\pi}{180}\right)^2 \mathbf{I} & 0 \\ 0 & 10^{-10}\mathbf{I} \end{bmatrix}, \qquad \textbf{(72)}$$

where $\Delta T = 1\text{s}$.

With these values, the steady-state Kalman gains (corresponding to $\boldsymbol{\omega} \equiv \boldsymbol{\theta}$) are given by

$$\begin{aligned} k_p &= 2\bar{k}_p = 6.9223 \times 10^{-2}, \\ k_b &= 5.7296 \times 10^{-4}. \end{aligned} \qquad \textbf{(73)}$$

The gyro attitude estimate is arbitrarily chosen to be the quaternion, and as such is obtained by propagating the equation

$$\begin{aligned} &\begin{bmatrix} \dot{\hat{\boldsymbol{q}}} \\ \dot{q}_4 \end{bmatrix} = \frac{1}{2} \begin{bmatrix} \hat{\boldsymbol{q}}^\times + q_4 I \\ -\boldsymbol{q}^T \end{bmatrix} \left(\boldsymbol{\omega}^m - \hat{\boldsymbol{b}} + \boldsymbol{u}_p \right), \ \textit{Case } (a), \\ &\begin{bmatrix} \dot{\hat{\boldsymbol{q}}} \\ \dot{q}_4 \end{bmatrix} = \frac{1}{2} \begin{bmatrix} \hat{\boldsymbol{q}}^\times + q_4 I \\ -\boldsymbol{q}^T \end{bmatrix} \delta \mathbf{C}^{GM}(t_k) \left(\boldsymbol{\omega}^m - \hat{\boldsymbol{b}} + \boldsymbol{u}_p \right), \ \textit{Case } (b), \\ &\dot{\hat{\boldsymbol{b}}} = -\boldsymbol{u}_b, \\ &\boldsymbol{u}_p(t) = -k_p \boldsymbol{y}(t_k), \ t_k \le t < t_{k+1}, \\ &\boldsymbol{u}_b(t) = -k_b \boldsymbol{y}(t_k), \ t_k \le t < t_{k+1}. \end{aligned} \qquad \textbf{(74)}$$

where

$$\boldsymbol{y} = \boldsymbol{\varepsilon}_{GM} \, sign(\eta_{GM}), \qquad \textbf{(75)}$$

and $\left(\boldsymbol{\varepsilon}_{GM}, \eta_{GM}\right)$ is a quaternion parameterizing $\delta \mathbf{C}^{GM}$.

The true initial attitude is given by the quaternion $\begin{bmatrix} \boldsymbol{q}_0^T & q_{40} \end{bmatrix}^T = \begin{bmatrix} 0 & 0 & 0 & 1 \end{bmatrix}^T$. The initial attitude estimate error is given by $\boldsymbol{\varepsilon}_0 = \frac{\sin(\pi/3)}{\sqrt{3}} \begin{bmatrix} 1 & 1 & -1 \end{bmatrix}^T$ with $sign(\eta_0) = 1$, and the initial gyro bias estimate is $\hat{\boldsymbol{b}}_0 = \begin{bmatrix} 0 & 0 & 0 \end{bmatrix}^T$ deg/s.

Figures 1 and 2 show the time histories of the attitude estimation errors and the gyro bias estimates. From these figures, it is clear that as predicted, the implementation of case (b) is more sensitive to measurement noise compared with case (a). Figure 3 shows the traces of the steady-state error covariances $\mathbf{P}_{\varepsilon\varepsilon,a}(t)$ and $\mathbf{P}_{bb,a}(t)$ compared with the corresponding traces of the steady-state error covariances for zero angular velocity (which are optimal in that case). It can be seen that the deterioration in performance is not significant, and similar performance is obtained compared to the optimal (zero angular velocity).

VII. Conclusion

In conclusion, a simple sub-optimal Kalman filter implementation requiring only two constant scalar gains has been presented for the gyro corrected attitude determination problem. The simplicity of the filter makes it computationally inexpensive to implement. This is particularly attractive for such applications where the computational power is limited, e.g. as in the cases of micro-/nano-satellite missions. The filter exhibits global stability with exponential convergence. When the satellite angular velocity is zero, the filter gains can be selected optimally as in the Kalman filter. It is shown that when the angular velocity is non-zero, the filter exhibits near optimal steady-state performance when compared with the zero-angular velocity case.

VIII. Acknowledgements

The author gratefully acknowledges the valuable discussions and feedback from James Lee, Yuri Kim and Alfred Ng of the Canadian Space Agency.

IX. References

[1] Y. Kim, A. De Ruiter, J. Lee, A. Ng, "Robust Implementation of Kalman Filter for INS Correction", *Actual Problems of Aviation and Aerospace Systems: Processes, Models, Experiment*, No. 3 (25), vol. 12, 2007.

[2] E. J. Lefferts, F. L. Markley, M. D. Shuster, "Kalman Filtering for Spacecraft Attitude Determination," *AIAA Journal of Guidance,* Vol. 5, No. 5, Sept.-Oct. 1982, pp. 417-429.

[3] J. L. Crassidis, F. L. Markley and Y. Cheng, "Survey of Nonlinear Attitude Estimation Methods", *AIAA Journal of Guidance, Control and Dynamics*, vol. 30, No. 1, January-February 2007, pp. 12-28.

[4] A. Ng, K. Yoshihara, H. Hashimoto, L. Ngo-Phong, B. S. Kumar, A. de Ruiter, " Nanosatellite Mission For Demonstrating Formation Keeping Technology With Aerodynamic Drag," 11th International Space Conference of Pacific basin Societies (ISCOPS), Beijing, China, 16-18 May, 2007.

[5] J. Thienel and R. M. Sanner, "A Coupled Nonlinear Spacecraft Attitude Controller and Observer With an Unknown Constant Gyro Bias and Gyro Noise", *IEEE Transactions on Automatic Control*, Vol. 48, No. 11, November 2003.

[6] J. K. Thienel and R. M. Sanner, "Hubble Space Telescope Angular Velocity Estimation During the Robotic Servicing Mission", *AIAA Journal of Guidance, Control and Dynamics*, vol. 30, No. 1, January-February 2007, pp. 29-34.

[7] S. Salcudean, "A Globally Convergent Angular Velocity Observer for Rigid Body Motion", *IEEE Transactions on Automatic Control*, Vol. 36, No. 12, December 1991.

[8] J. R. Wertz, *Spacecraft Attitude Determination and Control*, Dordrecht, Holland: Kluwer Academic Publishers, 1978.

[9] M. D. Shuster and S. D. Oh, "Three-Axis Attitude Determination from Vector Observations", *AIAA Journal of Guidance and Control*, Vol. 4, No. 1, Jan-Feb, 1981, pp. 70-77.

[10] C.E. Cohen, "Attitude Determination," *Global Positioning System: Theory and Applications*, Vol. II, edited by B. W. Parkinson and J. J. Spilker, Jr., AIAA, Washington, DC, 1996, pp. 519-538.

[11] P. C. Hughes, *Spacecraft Attitude Dynamics*. New York: Dover Publications, 2004.

[12] M. D. Shuster, "A Survey of Attitude Representations", *The Journal of the Astronautical Sciences*, Vol. 41, No. 4, Oct.-Dec. 1993, pp. 439-573.

[13] R. L. Farrenkopf, "Analytic Steady-State Accuracy Solutions for Two Common Spacecraft Attitude Estimators", *AIAA Journal of Guidance and, Control*, vol. 1, No. 4, 1978, pp. 282-284.

[14] F. L. Markley, "Attitude Error Representations for Kalman Filtering," *AIAA Journal of Guidance, Control and Dynamics*, vol. 26, No. 2, March-April 2003, pp. 311-317.

[15] D. Simon, *Optimal State Estimation*, John Wiley and Sons, New Jersey, 2006.

[16] A. Gelb, *Applied Optimal Estimation*, Cambridge, Massachusetts: The M.I.T. Press, 1974.

[17] A. N. Kolmogorov and S. V. Fomin, *Introductory Real Analysis*, Dover Publications, New York, 1975.

[18] H. Khalil, *Nonlinear Systems*, 2nd Ed., Prentice-Hall, Upper Saddle River, NJ, 1995.

[19] J. P. Lasalle, "An Invariance Principle in the Theory of Stability," in *Control Theory, Twenty-Five Seminal Papers (1932-1981)*, T. Basar, Ed. New York: IEEE Press, 2001, pp. 309-320.

[20] P. A. Ioannou and J. Sun, *Robust Adaptive Control*, Prentice-Hall, Upper Saddle River, New Jersey, 1995.

X. Appendix

A. Nomenclature

$\boldsymbol{a}$ = principal axis of rotation
$\mathbf{A}$ = system matrix
$\boldsymbol{b}_{\omega}$ = gyro measurement bias vector
$\hat{\boldsymbol{b}}_{\omega}$ = gyro measurement bias estimate
$\tilde{\boldsymbol{b}}_{\omega}$ = gyro measurement estimate error
$\mathbf{C}$ = rotation matrix
$\mathbf{C}_{bI}$ = rotation matrix representing the true spacecraft attitude
$\hat{\mathbf{C}}_{bI}^{M}$ = rotation matrix representing the external spacecraft attitude measurement
$\hat{\mathbf{C}}_{bI}^{G}$ = rotation matrix representing the gyro spacecraft attitude estimate
$\delta\mathbf{C}^{M}$ = rotation matrix representing the external attitude measurement error
$\delta\mathbf{C}^{G}$ = rotation matrix representing the true gyro attitude estimate error
$\delta\mathbf{C}^{GM}$ = rotation matrix representing the measured gyro attitude estimate error
$\mathbf{G}$ = process noise sensitivity matrix
$\mathbf{H}$ = measurement sensitivity matrix
$\mathbf{I}$ = identity matrix
k = scalar filter gain
$\mathbf{K}$ = filter gain matrix
$\mathbf{P}$ = gyro error covariance matrix
$\mathbf{P}_{ss}$ = steady-state gyro error covariance matrix
$(\boldsymbol{q}, q_4)$ = quaternion parameterization of the true spacecraft attitude, $\mathbf{C}_{bI}$
$(\hat{\boldsymbol{q}}, \hat{q}_4)$ = quaternion parameterization of the gyro spacecraft attitude estimate, $\hat{\mathbf{C}}_{bI}^{G}$
q = process noise scalar

$\mathbf{Q}$ = process noise covariance matrix
r = measurement noise scalar
$\mathbf{R}$ = measurement noise covariance matrix
$\mathbf{S}(\boldsymbol{\varepsilon},\eta)$ = attitude kinematics matrix associated with the quaternion $(\boldsymbol{\varepsilon},\eta)$
t_k = kth sample time
t^* = switching time
ΔT = sample period
$\boldsymbol{u}$ = gyro correction parameter
$\mathbf{W}(\boldsymbol{\alpha})$ = rotational kinematic matrix corresponding to the vector parameterization, $\boldsymbol{\alpha}$
$\boldsymbol{v}_M$ = external measurement noise
$\boldsymbol{w}_\omega$ = gyro measurement noise vector
$\boldsymbol{y}$ = filter input
$\boldsymbol{\alpha}$ = any vector parameterization of the true attitude $\mathbf{C}_{bI}$
$\hat{\boldsymbol{\alpha}}$ = any vector parameterization of the gyro spacecraft attitude estimate, $\hat{\mathbf{C}}_{bI}^{G}$
$(\boldsymbol{\varepsilon},\eta)$ = quaternion parameterization of the gyro attitude estimate error, $\delta\mathbf{C}^{G}$
$(\boldsymbol{\varepsilon}_{GM},\eta_{GM})$ = quaternion parameterization of the measured gyro attitude estimate error, $\delta\mathbf{C}^{GM}$
$(\boldsymbol{\varepsilon}_{M},\eta_{M})$ = quaternion parameterization of the external attitude measurement error, $\delta\mathbf{C}^{M}$
ϕ = principal angle of rotation
$\boldsymbol{\omega}$ = spacecraft angular velocity vector expressed in body coordinates
$\boldsymbol{\omega}^m$ = measured angular velocity vector
$\bar{\boldsymbol{\omega}}$ = propagated angular velocity vector
$\delta\boldsymbol{\omega}$ = angular velocity error vector expressed in frame $\Im_b^G$
$\boldsymbol{\Phi}$ = state-transition matrix
σ = scalar covariance (positive)
$\Im_b$ = true spacecraft body frame
$\Im_b^G$ = gyro estimate of the spacecraft body frame

B. Proof of Theorem 1

Consider the closed-loop equations given by (36).

Let the system have arbitrary initial conditions $\boldsymbol{\varepsilon}(0),\eta(0),\ \tilde{\boldsymbol{b}}_\omega(0)$ with $\boldsymbol{\varepsilon}^T(0)\boldsymbol{\varepsilon}(0)+\eta(0)^2=1$. Solutions obtained by integrating equation (31) are absolutely continuous on any finite interval $[0,t]$ where $t<\infty$ [17]. Consider the function $T=\boldsymbol{\varepsilon}^T\boldsymbol{\varepsilon}+\eta^2$. Since on any closed finite interval T is a sum of products of absolutely continuous functions, it too is absolutely continuous on any finite interval $[0,t]$ where $t<\infty$. Since it is absolutely-continuous, it is differentiable almost everywhere with derivative $\dot{T}$, and $T(t)=T(0)+\int_0^t \dot{T}(\tau)d\tau$ [17]. Taking the derivative of T along the trajectories of (31) gives $\dot{T}\equiv 0$ almost everywhere. Therefore, $\boldsymbol{\varepsilon}(t)^T\boldsymbol{\varepsilon}(t)+\eta(t)^2=1,\ \ t\geq 0$. In particular, this means that $\boldsymbol{\varepsilon}(t)^T\boldsymbol{\varepsilon}(t)\leq 1,\ \ t\geq 0$ and $\eta(t)^2\leq 1,\ t\geq 0$.

Consider the function

$$V(\boldsymbol{\varepsilon},\eta,\tilde{\boldsymbol{b}}_\omega)=2\left(1-|\eta|\right)+\frac{\tilde{\boldsymbol{b}}_\omega^T\mathbf{K}_b^{-1}\tilde{\boldsymbol{b}}_\omega}{2}. \quad \textbf{(76)}$$

Given the above reasoning that $\eta(t)^2 \le 1,\ t\ge 0$, $V(\boldsymbol{\varepsilon},\eta,\tilde{\boldsymbol{b}}_\omega)$ is positive semi-definite over its domain. Now, the absolute value of an absolutely continuous function is itself also absolutely continuous, and on any closed finite interval, a quadratic form of absolutely continuous functions being the sum of products of absolutely continuous functions is also absolutely continuous. Therefore, along the trajectories of (31), the function $V(\boldsymbol{\varepsilon},\eta,\tilde{\boldsymbol{b}}_\omega)$ is also an absolutely continuous function of time for any finite interval $[0,t]$ where $t<\infty$. As such, it is differentiable almost everywhere, and $V(\boldsymbol{\varepsilon}(t),\eta(t),\tilde{\boldsymbol{b}}_\omega(t))=V(\boldsymbol{\varepsilon}(0),\eta(0),\tilde{\boldsymbol{b}}_\omega(0))+\int_0^t \dot{V}(\tau)d\tau$. The derivatives of $V(\boldsymbol{\varepsilon},\eta,\tilde{\boldsymbol{b}}_\omega)$ along the trajectories of (31) are now examined. An examination of (121) shows that the function $V(\boldsymbol{\varepsilon},\eta,\tilde{\boldsymbol{b}}_\omega)$ is differentiable with respect to $(\boldsymbol{\varepsilon},\eta,\tilde{\boldsymbol{b}}_\omega)$ provided $\eta\neq 0$. From (31), it is clear that the trajectories of the system are also differentiable when $\eta\neq 0$. Performing the differentiation in these cases leads to $\dot{V}=-\boldsymbol{\varepsilon}^T\mathbf{K}_p\boldsymbol{\varepsilon}\le 0$. At the times when the trajectories are such that η crosses from $|\eta|>0$ into $\eta=0$ or vice-versa, the trajectories are not differentiable as seen from (31), and the set of these times has measure zero. The final case to be considered is when $\eta=0$ on a non-zero interval of time. Over this interval, $V(\boldsymbol{\varepsilon},\eta,\tilde{\boldsymbol{b}}_\omega)=\frac{\tilde{\boldsymbol{b}}_\omega^T\mathbf{K}_b^{-1}\tilde{\boldsymbol{b}}_\omega}{2}$, with derivative given by $\dot{V}=-\tilde{\boldsymbol{b}}_\omega^T\boldsymbol{\varepsilon}$. Since $\dot{\eta}=0$ on this interval, (31) gives that $\tilde{\boldsymbol{b}}_\omega^T\boldsymbol{\varepsilon}=\boldsymbol{\varepsilon}^T\mathbf{K}_p\boldsymbol{\varepsilon}$, and hence $\dot{V}=-\boldsymbol{\varepsilon}^T\mathbf{K}_p\boldsymbol{\varepsilon}\le 0$. Therefore, it can be concluded that

$$\dot{V}=-\boldsymbol{\varepsilon}^T\mathbf{K}_p\boldsymbol{\varepsilon}\le 0 \quad \textbf{(77)}$$

almost everywhere. This leads to the inequality

$$V(\boldsymbol{\varepsilon}(t),\eta(t),\tilde{\mathbf{b}}_\omega(t))\le V(\boldsymbol{\varepsilon}(0),\eta(0),\tilde{\mathbf{b}}_\omega(0)),\ t\ge 0\,. \quad \textbf{(78)}$$

Inequality (78) implies that $\tilde{\mathbf{b}}_\omega(t)$ is bounded. Since $\boldsymbol{\omega}(t)$ is bounded (by assumption), (31) gives that $\dot{\boldsymbol{\varepsilon}}(t),\dot{\eta}(t),\ddot{\tilde{\mathbf{b}}}_\omega(t)$ are bounded almost everywhere. Therefore, it can be concluded that $\boldsymbol{\varepsilon}(t),\eta(t),\tilde{\mathbf{b}}_\omega(t)$ are uniformly continuous. Now, consider the function

$$W(t)=\boldsymbol{\varepsilon}^T(t)\mathbf{K}_p\boldsymbol{\varepsilon}(t)\ge 0\,. \quad \textbf{(79)}$$

Since $\boldsymbol{\varepsilon}(t)$ is uniformly continuous and bounded, $W(t)$ is uniformly continuous also. Furthermore, (77) gives that $W(t)=-\dot{V}(t)$ almost everywhere. Therefore,

$$\int_0^t W(\tau)d\tau = -\int_0^t \dot{V}(\tau)d\tau = V(\boldsymbol{\varepsilon}(0),\eta(0),\tilde{\boldsymbol{b}}_\omega(0)) - V(\boldsymbol{\varepsilon}(t),\eta(t),\tilde{\boldsymbol{b}}_\omega(t)) \le V(\boldsymbol{\varepsilon}(0),\eta(0),\tilde{\boldsymbol{b}}_\omega(0)). \quad \textbf{(80)}$$

Letting $t \to \infty$, $\int_0^\infty W(\tau)d\tau \le V(\boldsymbol{\varepsilon}(0),\eta(0),\tilde{\boldsymbol{b}}_\omega(0))$, and upon application of Barbalat's Lemma [18], $W(t) \to 0$ as $t \to \infty$. From (79), this implies that $\boldsymbol{\varepsilon}(t) \to 0$ as $t \to \infty$.

The non-autonomous component of the right hand side of (31) is given by the term $\boldsymbol{\omega}^\times\boldsymbol{\varepsilon}$. Since $\boldsymbol{\omega}$ is bounded, we have $\left\|\boldsymbol{\omega}^\times\boldsymbol{\varepsilon}\right\| \to 0$ as $t \to \infty$, i.e. the closed-loop system equations become time independent as $t \to \infty$. Thus, along the considered trajectory $\boldsymbol{\varepsilon}(t),\eta(t),\tilde{\boldsymbol{b}}_\omega(t)$, the closed-loop system is asymptotically autonomous to the system

$$\begin{aligned}
\dot{\boldsymbol{\varepsilon}} &= \mathbf{S}(\boldsymbol{\varepsilon},\eta)\left(\tilde{\boldsymbol{b}}_\omega - \mathbf{K}_p\boldsymbol{\varepsilon}sign(\eta)\right),\\
\dot{\eta} &= -\frac{1}{2}\boldsymbol{\varepsilon}^T\left(\tilde{\boldsymbol{b}}_\omega - \mathbf{K}_p\boldsymbol{\varepsilon}sign(\eta)\right),\\
\dot{\tilde{\boldsymbol{b}}}_\omega &= -\mathbf{K}_b\boldsymbol{\varepsilon}sign(\eta).
\end{aligned} \quad (81)$$

A property of asymptotically autonomous systems is that the positive limit set is invariant under the system that it is asymptotically autonomous to [19]. This means that the positive limit set of the trajectory is invariant under (81), and this means that the states $\boldsymbol{\varepsilon}(t),\eta(t),\tilde{\boldsymbol{b}}_\omega(t)$ approach an invariant set of (81) as $t \to \infty$. Define the set *M* as the largest invariant set of (81) such that $\boldsymbol{\varepsilon}(t) \equiv \boldsymbol{0}$. This set is given by $M = \left\{(\boldsymbol{\varepsilon}(t),\eta(t),\tilde{\boldsymbol{b}}_\omega(t)) : \boldsymbol{\varepsilon} = 0, \eta = \pm 1, \tilde{\boldsymbol{b}}_\omega = 0\right\}$. Therefore, it is concluded that $\boldsymbol{\varepsilon}(t),\eta(t),\tilde{\boldsymbol{b}}_\omega(t)$ approaches the set *M* and hence $\tilde{\mathbf{b}}_\omega \to 0$ as $t \to \infty$ also. This concludes the proof.

C. Proof of Theorem 2

From the proof of Theorem 1, $\boldsymbol{\varepsilon}(t)^T\boldsymbol{\varepsilon}(t) + \eta(t)^2 = 1, \quad t \ge 0$, and therefore the function (76) can also be written as

$$V(\boldsymbol{\varepsilon},\eta,\tilde{\boldsymbol{b}}_\omega) = 2\left(1 - \left(1 - \boldsymbol{\varepsilon}^T\boldsymbol{\varepsilon}\right)^{\frac{1}{2}}\right) + \frac{\boldsymbol{b}_\omega^T\mathbf{K}_b^{-1}\tilde{\boldsymbol{b}}_\omega}{2}. \quad \textbf{(82)}$$

Restricting $\mathbf{K}_p = k_p\mathbf{I}$, the proof of theorem 1 gives

$$\dot{V} = -k_p\boldsymbol{\varepsilon}^T\boldsymbol{\varepsilon} \le 0, \quad \textbf{(83)}$$

almost everywhere, $\boldsymbol{\varepsilon}(t),\eta(t),\tilde{\boldsymbol{b}}_\omega(t)$ are uniformly continuous with $\boldsymbol{\varepsilon}(t) \to 0$ as $t \to \infty$. Define the vector

$\boldsymbol{x} = \begin{bmatrix} \boldsymbol{\varepsilon} \\ \tilde{\boldsymbol{b}}_\omega \end{bmatrix}$. Now, some bounds on $V(\boldsymbol{x})$ will be obtained. First, note that

$$\frac{1}{2\lambda_{\max}(\mathbf{K}_b)}\left\|\tilde{\boldsymbol{b}}_\omega\right\|^2 \le \frac{\tilde{\boldsymbol{b}}_\omega^T\mathbf{K}_b^{-1}\tilde{\boldsymbol{b}}_\omega}{2} \le \frac{1}{2\lambda_{\min}(\mathbf{K}_b)}\left\|\tilde{\boldsymbol{b}}_\omega\right\|^2. \quad \textbf{(84)}$$

It can be shown after some work that

$$\frac{1}{2}\|\boldsymbol{\varepsilon}\|^2 \le \left(1-\left(1-\boldsymbol{\varepsilon}^T\boldsymbol{\varepsilon}\right)^{\frac{1}{2}}\right) \le \|\boldsymbol{\varepsilon}\|^2, \quad \|\boldsymbol{\varepsilon}\| \le 1 \quad \textbf{(85)}$$

Finally, the following inequality is obtained

$$c_1\|\boldsymbol{x}\|^2 \le V(\boldsymbol{x}) \le c_2\|\boldsymbol{x}\|^2, \quad \textbf{(86)}$$

where $c_1 = \min\left(1, \frac{1}{2\lambda_{\max}(\mathbf{K}_b)}\right)$ and $c_2 = \max\left(2, \frac{1}{2\lambda_{\min}(\mathbf{K}_b)}\right)$. The remainder of the proof proceeds almost identically to the proof of Theorem 1 in [5]. First, we note that (83) may be rewritten as

$$\dot{V} = -k_p\boldsymbol{x}\mathbf{H}^T\mathbf{H}\boldsymbol{x}, \quad \textbf{(87)}$$

where $\mathbf{H} = \begin{bmatrix}\mathbf{I} & \mathbf{0}\end{bmatrix}$. Second, making use of (36) along the considered trajectory, the trajectory satisfies the linear time-varying system given by

$$\dot{\boldsymbol{x}} = \mathbf{A}(t)\boldsymbol{x}, \quad \textbf{(88)}$$

where

$$\mathbf{A}(t) = \begin{bmatrix} -\boldsymbol{\omega}^\times - \mathbf{S}(\boldsymbol{\varepsilon},\eta)k_p sign(\eta) & \mathbf{S}(\boldsymbol{\varepsilon},\eta) \\ -\mathbf{K}_b sign(\eta) & \mathbf{0} \end{bmatrix}. \quad \textbf{(89)}$$

Since $\boldsymbol{\omega}$ and $\boldsymbol{\varepsilon},\eta$ are bounded (as has already been established in the proof of theorem 1), this system is well-defined. Now, let $\boldsymbol{\Phi}(\tau,t)$ be the state-transition matrix for the system (89). The existence of $\delta > 0$ and $\bar{k} > 0$ are sought such that for all $t \ge 0$, $\int_t^{t+\delta} \dot{V}dt \le -\bar{k}\|\boldsymbol{x}(t)\|^2$. It is shown in [18], that this is can be obtained by demonstrating the Uniform Observability of the pair $\left(\mathbf{A}(t), \mathbf{H}\right)$, which means that there exists a $\delta > 0$ and $k > 0$ such that for all $t \ge 0$, such that

$$\int_t^{t+\delta} \boldsymbol{\Phi}^T(\tau,t)\mathbf{H}^T\mathbf{H}\boldsymbol{\Phi}(\tau,t)d\tau \ge k\mathbf{I}. \quad \textbf{(90)}$$

From Lemma 4.8.1 in [20], this is equivalent to the Uniform Observability of the pair $\left(\mathbf{A}(t)-\mathbf{K}(t)\mathbf{H}, \mathbf{H}\right)$, where there exist constant $k_K > 0$ such that for all $t \ge 0$, $\mathbf{K}(t)$ satisfies

$$\int_t^{t+\delta} \|\mathbf{K}(\tau)\|^2 d\tau \le k_K. \quad \textbf{(91)}$$

Similarly to [5], choose

$$\mathbf{K}(t) = \begin{bmatrix} \mathbf{S}(\boldsymbol{\varepsilon},\eta)k_p sign(\eta) \\ \mathbf{K}_b sign(\eta) \end{bmatrix}. \quad \textbf{(92)}$$

By the boundedness and continuity of $\boldsymbol{\varepsilon},\eta$, the matrix $\mathbf{K}(t)$ satisfies (91) for some $k_K(\delta)>0$. Therefore, the uniform observability of the pair $\left(\bar{\mathbf{A}}(t),\mathbf{H}\right)$ is sought, where $\bar{\mathbf{A}}(t)=\begin{bmatrix}-\boldsymbol{\omega}^{\times} & \mathbf{S}(\boldsymbol{\varepsilon},\eta)\\ \mathbf{0} & \mathbf{0}\end{bmatrix}$. Let $\mathbf{C}(t)$ be a rotation matrix satisfying the equation $\dot{\mathbf{C}}=-\boldsymbol{\omega}^{\times}\mathbf{C}$. Then, the state-transition matrix corresponding to $\bar{\mathbf{A}}(t)$ can be found to be

$$\bar{\boldsymbol{\Phi}}(\tau,t)=\begin{bmatrix}\mathbf{C}(\tau)\mathbf{C}^T(t) & \int_t^{\tau}\mathbf{C}(\tau)\mathbf{C}^T(s)\mathbf{S}(\boldsymbol{\varepsilon}(s),\eta(s))ds\\ 0 & \mathbf{I}\end{bmatrix}. \tag{93}$$

Now, uniform observability of the pair $\left(\bar{A}(t),H\right)$ can be determined by establishing the existence of $\delta>0$ and $k_1>0$ such that for all $t\geq 0$,

$$\int_t^{t+\delta}\bar{\boldsymbol{\Phi}}^T(\tau,t)\mathbf{H}^T\mathbf{H}\bar{\boldsymbol{\Phi}}(\tau,t)d\tau\geq k_1\mathbf{I}. \tag{94}$$

Defining the functions $\boldsymbol{\theta}(s,t)=\mathbf{C}(t)\mathbf{C}^T(s)\mathbf{S}(\boldsymbol{\varepsilon}(s),\eta(s))$ and $\boldsymbol{\psi}(\tau,t)=\int_t^{\tau}\boldsymbol{\theta}(s,t)ds$, the integrand in (94) can be written as

$$\bar{\boldsymbol{\Phi}}^T(\tau,t)\mathbf{H}^T\mathbf{H}\bar{\boldsymbol{\Phi}}(\tau,t)=\begin{bmatrix}\mathbf{I} & \boldsymbol{\psi}(\tau,t)\\ \boldsymbol{\psi}^T(\tau,t) & \boldsymbol{\psi}^T(\tau,t)\boldsymbol{\psi}(\tau,t)\end{bmatrix}. \tag{95}$$

Note that $\boldsymbol{\theta}(s,t)$ is an absolutely continuous function, and as such is differentiable almost everywhere. From the proof of Lemma 13.4 in [18], in order to establish the existence of a $\delta>0$ and $k_1>0$ such that (94) holds for all $t\geq 0$, it is sufficient to establish the boundedness of $\boldsymbol{\theta}(s,t)$ and $\dfrac{d\boldsymbol{\theta}(s,t)}{ds}$, and find $\delta_2>0$ and $k_2>0$ such that for all $t\geq 0$,

$$\int_t^{t+\delta_2}\boldsymbol{\theta}^T(s,t)\boldsymbol{\theta}(s,t)ds\geq k_2\mathbf{I}. \tag{96}$$

Now, $\boldsymbol{\theta}^T(s,t)\boldsymbol{\theta}(s,t)=\mathbf{S}^T(\boldsymbol{\varepsilon}(s),\eta(s))\mathbf{S}(\boldsymbol{\varepsilon}(s),\eta(s))=\mathbf{I}-\boldsymbol{\varepsilon}\boldsymbol{\varepsilon}^T$. Just as in [5], it is established that $\boldsymbol{\varepsilon}\to\boldsymbol{\theta}$, and therefore, given a $\beta>0$ there is a time T_1 such that $\|\boldsymbol{\varepsilon}\|<\beta$ for all $t\geq T_1$, in particular, it also holds for all time $t\geq\tau+T_1$, with $\tau\geq 0$. Choose a time $T_2>T_1$, and an arbitrary vector $\boldsymbol{z}\in R^3$ and consider the quantity $\boldsymbol{z}^T\int_t^{t+T_2}\boldsymbol{\theta}^T(s,t)\boldsymbol{\theta}(s,t)ds\boldsymbol{z}$.This gives

$$\boldsymbol{z}^T \int_t^{t+T_2} \boldsymbol{\theta}^T(s,t)\boldsymbol{\theta}(s,t)ds\boldsymbol{z} \geq \boldsymbol{z}^T \int_{t+T_1}^{t+T_2} \boldsymbol{\theta}^T(s,t)\boldsymbol{\theta}(s,t)ds\boldsymbol{z}$$

$$= \boldsymbol{z}^T\boldsymbol{z}\left(T_2 - T_1\right) - \boldsymbol{z}^T \int_{t+T_1}^{t+T_2} \boldsymbol{\varepsilon}(s)\boldsymbol{\varepsilon}^T(s)ds\boldsymbol{z} \qquad \textbf{(97)}$$

$$\geq \boldsymbol{z}^T\boldsymbol{z}\left(T_2 - T_1\right)\left(1-\beta^2\right).$$

Hence, for a given $0 < \beta < 1$, inequality (96) holds with $\delta_2 = T_2$ and $k_2 = (T_2 - T_1(\beta))\left(1-\beta^2\right)$. The boundedness of $\boldsymbol{\theta}(s,t)$ follows from the boundedness of $\boldsymbol{\varepsilon}, \eta, \mathbf{C}(t)$. Now, taking the derivative of $\boldsymbol{\theta}(s,t)$ gives

$$\frac{d\boldsymbol{\theta}(s,t)}{ds} = \mathbf{C}(t)\mathbf{C}^T(s)\boldsymbol{\omega}^{\times}\mathbf{S}(\boldsymbol{\varepsilon}(s),\eta(s)) + \frac{1}{2}\mathbf{C}(t)\mathbf{C}^T(s)\left(\dot{\boldsymbol{\varepsilon}}^{\times} + \dot{\eta}\mathbf{I}\right), \qquad \textbf{(98)}$$

From (36), $\dot{\boldsymbol{\varepsilon}}, \dot{\eta}$ are bounded, and hence $\dfrac{d\boldsymbol{\theta}(s,t)}{ds}$ is bounded also. Therefore, inequality (90) holds for all $t \geq 0$ for some $\delta > 0$ and $k > 0$, which means that along the trajectory,

$$\int_t^{t+\delta} \dot{V}dt \leq -\bar{k}\left\|\boldsymbol{x}(t)\right\|^2, \quad t \geq 0 \qquad \textbf{(99)}$$

with $\bar{k} = k_p k$. Following the proof of Theorem 4.5 in [18], exponential convergence of the trajectory is concluded. Note that uniform exponential convergence cannot be claimed, since the constants $\delta > 0$ and $k > 0$, depend upon the trajectory.

D. Proof of Theorems 3 and 4

These are similar to the proofs for Theorems 1 and 2, except that the closed-loop system (equation (36)) is autonomous, and hence LaSalle's theorem [18] may be applied directly to obtain the result in Theorem 3, and in the proof of Theorem 4 the angular velocity is set to zero $\boldsymbol{\omega} \equiv \boldsymbol{\theta}$ (since the equations are independent of $\boldsymbol{\omega}$), the rotation matrix $\mathbf{C}(t)$ in the proof of Theorem 2 becomes the identity matrix, ie. $\mathbf{C}(t) = \mathbf{I}$ and the matrix $\mathbf{S}(\boldsymbol{\varepsilon}, \eta)$ is replaced by $\mathbf{S}(-\boldsymbol{\varepsilon}, \eta)$.

E. Figures

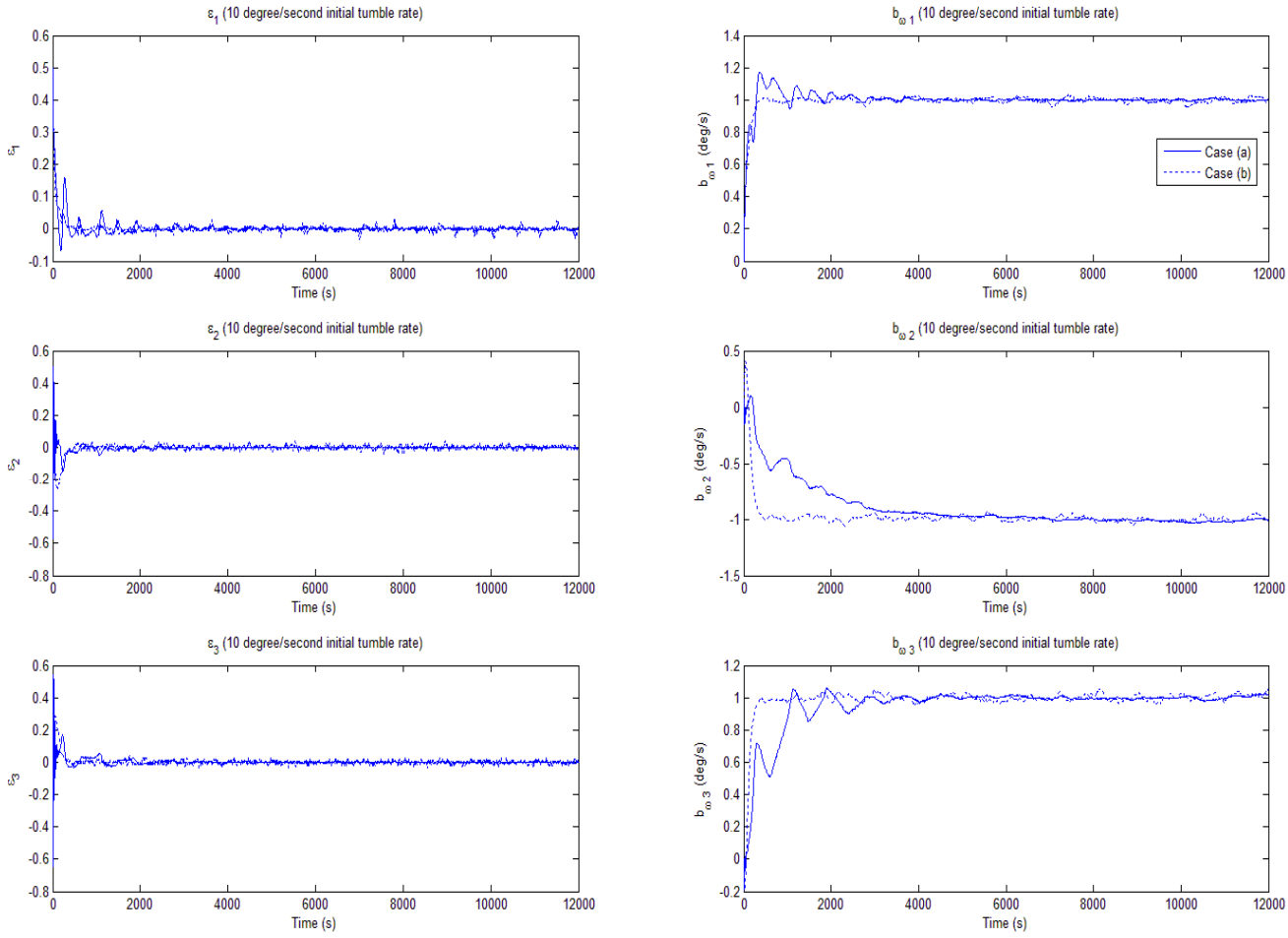

Figure 1: Transient Estimation Errors for an initial 10 degree/second satellite tumble rate

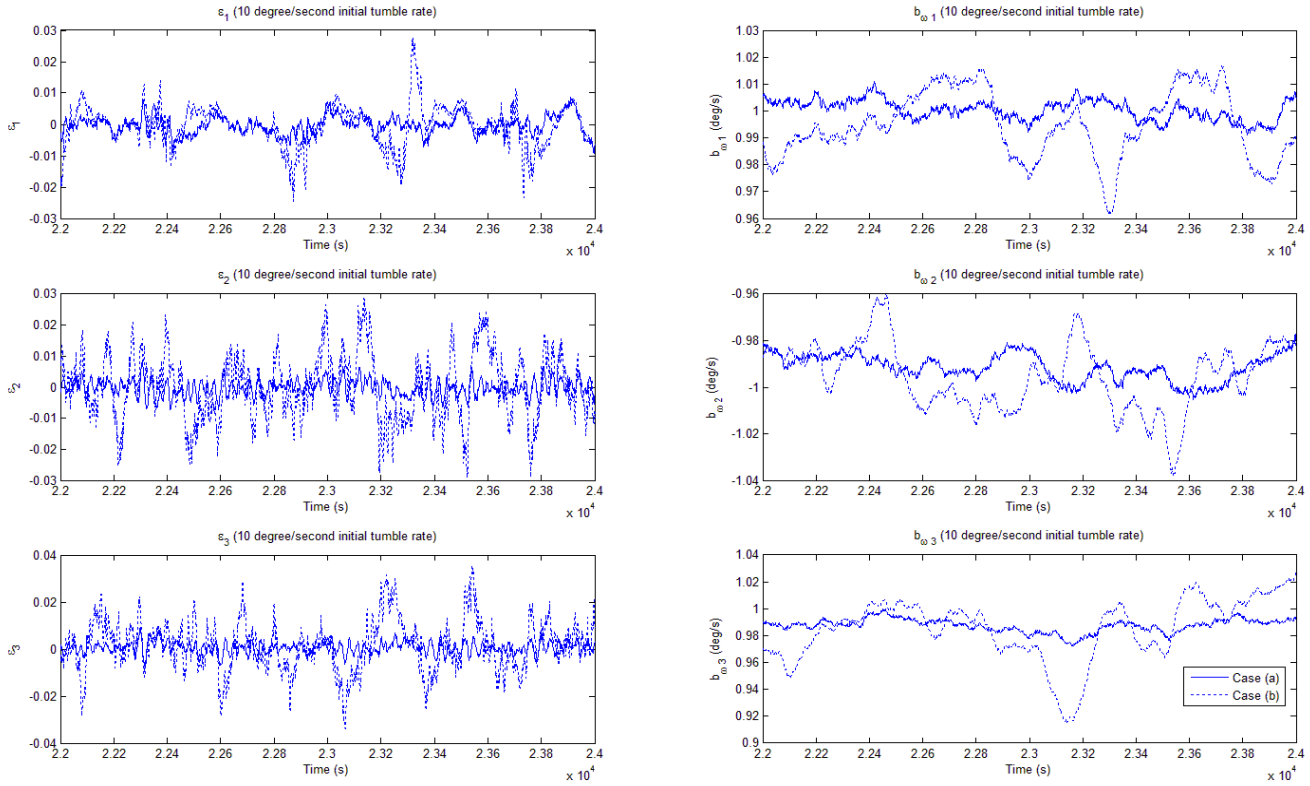

Figure 2: Steady-State Estimation Errors for an initial 10 degree/second satellite tumble rate

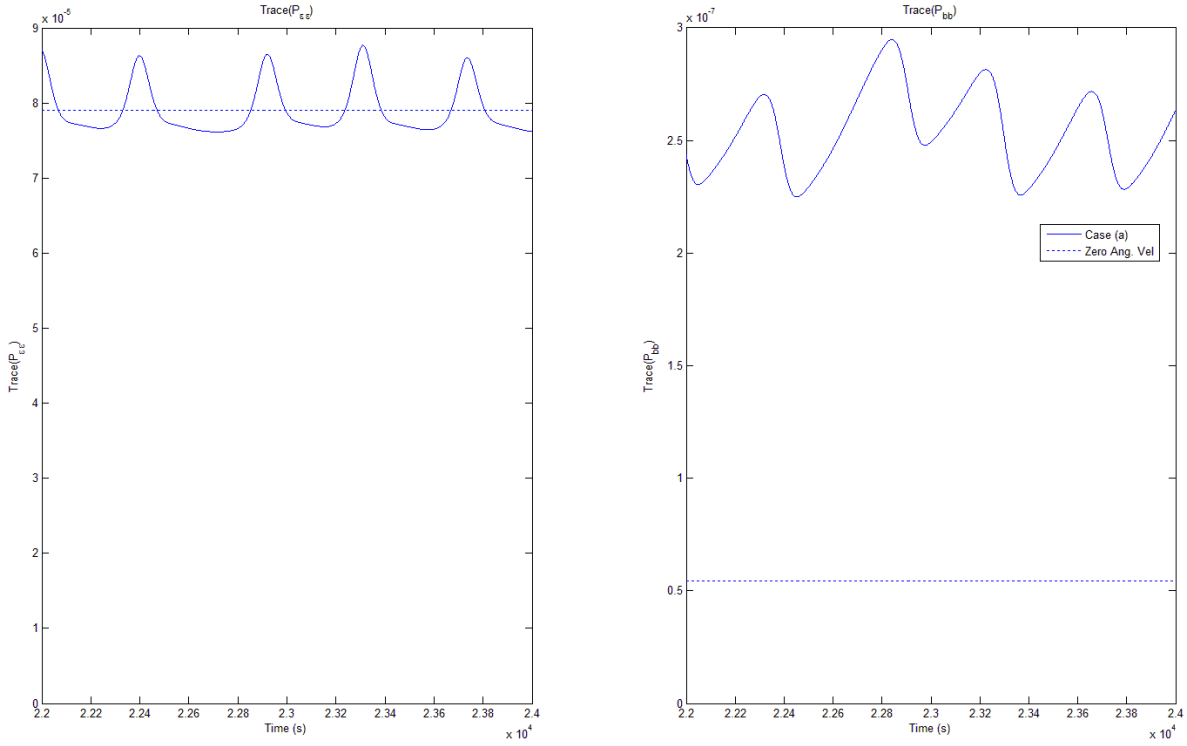

Figure 3: Steady-State Estimation Error Covariances